NTNU – Trondheim
Norwegian University of
Science and Technology

Measurements and Modelling of Hydrocarbon Dew Points for Natural Gases

Eirini Skylogianni

Natural Gas Technology
Submission date: May 2013
Supervisor: Even Solbraa, EPT
Co-supervisor: Efstathios Skouras Iliopoulos, Statoil
Epaminontas Voutsas, NTUA

Norwegian University of Science and Technology
Department of Energy and Process Engineering

NTNU
Norwegian University
of Science and Technology

Department of Energy
and Process Engineering

EPT-M-2012-143

MASTER THESIS

for

student Eirini Skylogianni

Autumn 2012

"Measurements and modelling of hydrocarbon dew points for natural gases"

Måling and modellering av hydrokarbonduggpunkt for naturgass

Background and objective

The knowledge of the hydrocarbon dew point (HCDP) is of great importance for the oil & gas industry as it is one of the gas quality specifications used for ensuring safe transport of natural gas. Avoiding hydrocarbon condensation is crucial as the presence of liquids in the pipelines increases the pressure drop and introduces operational problems in pipelines designed for single phase transportation. Thus, accurate measurement and prediction of hydrocarbon dew points are of great importance to obtain a safe and effective utilization of the natural gas pipelines.

At the laboratory facilities of Statoil in Trondheim a new rig (GERG rig) for measuring hydrocarbon dew points for natural gases is available. We are currently evaluating the effect of various factors, such as the filling procedure, the chamber temperature and the conditioning of the gas samples in the accuracy of the measurements.

Prediction of hydrocarbon dew point data in the oil & gas industry is usually done by thermodynamic models, such as traditional equations of state (EoS), like SRK and PR. Previous studies pointed out that classic EoS had difficulties in correctly representing the dew point line for natural gases, while more advanced models, such as the UMR-PRU significantly improve the predictions.

The following tasks are to be considered:

1. Literature review: Challenges with experimental determination and modelling of the HCDP for natural gases
2. Measurement of HCDP in the GERG rig. Effect of various factors such as the filling procedure and the chamber temperature.
3. Proposal of an operating procedure for reliable HCDP measurements in the GERG rig.
4. Modelling of hydrocarbon dew points with classic EoS and other models such the UMR-PRU.

Within 14 days of receiving the written text on the master thesis, the candidate shall submit a research plan for his project to the department.

When the thesis is evaluated, emphasis is put on processing of the results, and that they are presented in tabular and/or graphic form in a clear manner, and that they are analyzed carefully.

The thesis should be formulated as a research report with summary both in English and Norwegian, conclusion, literature references, table of contents etc. During the preparation of the text, the candidate should make an effort to produce a well-structured and easily readable report. In order to ease the evaluation of the thesis, it is important that the cross-references are correct. In the making of the report, strong emphasis should be placed on both a thorough discussion of the results and an orderly presentation.

The candidate is requested to initiate and keep close contact with his/her academic supervisor(s) throughout the working period. The candidate must follow the rules and regulations of NTNU as well as passive directions given by the Department of Energy and Process Engineering.

Risk assessment of the candidate's work shall be carried out according to the department's procedures. The risk assessment must be documented and included as part of the final report. Events related to the candidate's work adversely affecting the health, safety or security, must be documented and included as part of the final report. If the documentation on risk assessment represents a large number of pages, the full version is to be submitted electronically to the supervisor and an excerpt is included in the report.

Pursuant to "Regulations concerning the supplementary provisions to the technology study program/Master of Science" at NTNU §20, the Department reserves the permission to utilize all the results and data for teaching and research purposes as well as in future publications.

The final report is to be submitted digitally in DAIM. An executive summary of the thesis including title, student's name, supervisor's name, year, department name, and NTNU's logo and name, shall be submitted to the department as a separate pdf file. Based on an agreement with the supervisor, the final report and other material and documents may be given to the supervisor in digital format.

☐ Work to be done in lab (Water power lab, Fluids engineering lab, Thermal engineering lab)
☐ Field work

Department of Energy and Process Engineering, 16. January 2012

Olav Bolland
Department Head

Even Solbraa
Academic Supervisor

Research Advisors: Efstathios Skouras – Iliopoulos from Statoil Rotvoll

Acknowledgements

This project is based upon dew point measurements performed at Statoil Research Center in Trondheim. I would like to thank, first, everybody in Statoil for welcoming me and continuously motivating me.

Thanks to Kaja Klæbo Hjelseth for helping me with the experimental work.

Thanks to Toril Haugum for helping me with the GC analysis required for my thesis.

Thanks to Eleni Panteli for her support and guidance during this work.

Last but not least, I would like to express my gratitude to my supervisors in Statoil Efstathios Skouras-Iliopoulos and Even Solbraa as well as my supervisor at NTUA Epaminondas Voutsas for their guidance and great investment of time and energy in my work.

Abstract

The knowledge of the hydrocarbon dew point (HCDP) is of great importance for the oil and gas industry as it is one of the gas quality specifications used for ensuring safe transport of natural gas. Avoiding hydrocarbon condensation is crucial as the presence of liquids in the pipelines increases the pressure drop and introduces operational problems in pipelines designed for single phase transportation. Thus, accurate measurement and prediction of hydrocarbon dew points are of great importance to obtain a safe and effective utilization of the natural gas pipelines.

At the laboratory facilities of Statoil in Trondheim a new rig (GERG rig) for measuring hydrocarbon dew points for natural gases is available. Hydrocarbon dew points were measured in order to study the effect of various factors on the accuracy of the HCDP measurement and, therefore, perform the qualification of the GERG rig.

Hydrocarbon dew points are usually predicted using thermodynamic models, such as traditional cubic equations of state, like Soave-Redlich-Kwong (SRK). Previous studies have pointed out that classic EoS are not able to correctly represent the dew point line for natural gases, while more advanced models, such as the UMR-PRU, which is the Universal Mixing Rule combined with Peng Robinson Eos and UNIFAC, give significantly improved predictions.

In this diploma thesis, hydrocarbon dew point measurements have been performed for two synthetic gases and one real gas. Several experiments have been conducted in order to study the effect of the volume of the sample gas, the chamber's temperature and the sample conditioning. The results show that there is no volume effect or effect of the sample conditioning. On the other hand, a 10°C difference of the chamber's temperature from 35 to 45 °C has an effect of approximately 0.9 °C on the measured dew points. Given the fact that there is adsorption of heavy hydrocarbons inside the rig, which is a known challenge in HCDP measurements, the effect is more pronounced in gases consisting of heavier compounds, as in the case of the real gas.

The dew point experimental data are used to evaluate the reliability of three thermodynamic models: SRK, PC-SAFT and UMR-PRU.All three models studied appear to yield satisfactory results. SRK and PC-SAFT's predictions are very similar at low pressures up to the cricondentherm temperature, while SRK is better than PC-SAFT at higher pressures. Both these models describe better the experimental data obtained from the synthetic gases than UMR-PRU, except from the high pressures, and especially the cricondenbar pressure, where UMR-PRU gives the best results. Furthermore, the real gas' dew point curve is adequately predicted by UMR-PRU, which yields the best predictions than the other two models. Finally, an uncertainty analysis is performed which further confirms the reliability of the UMR-PRU model.

Table of Contents

List of Figures

List of Tables

Nomenclature

Latin Letters

A_{nm}, B_{nm}, C_{nm}	Interaction parameters of UNIFAC between groups n and m
α	Attractive parameter of a cubic EoS
b	Co-volume parameter of a cubic EoS
G	Gibbs free energy
K	Equilibrium constant
k	Interaction parameter
m	Parameter in α parameter of EoS
P	Pressure (*bar* refers to *bara*)
Q_k	Relative Van der Waals surface area of sub-group k
q_i	Relative Van der Waals surface area of compound i
R	Gas constant
r_i	Relative Van der Waals volume of compound i
T	Temperature
V	Volume
v	Molar volume
x	Molar fraction
Z	Compressibility factor

Greek letters

Γ_k	Residual activity coefficient of group k in a solution
θ_i	Surface area fraction of component i
θ	surface coverage
ϕ_i	Segment fraction of component i
Ψ	UNIFAC parameter
ω	Acentric factor

Superscripts

E	Excess property
res	Residual term
SG	Staverman–Guggenheim contribution

Subscripts

c	Critical
ij	Cross parameter (defined by the combining rules)
i(j)	Component in a mixture
r	Reduced property
cal	Calibration

Abbreviations

CCB	Cricondenbar Pressure
CCT	Cricondentherm Temperature
EoS	Equation of State
FID	Flame Ionization Detector
GC	Gas Chromatograph
GERG	European Gas Research Group
HCDP	Hydrocarbon Dew Point
PC-SAFT	Perturbed-Chain Statistical Associating Fluid Theory EoS
PFD	Process Flow Diagram
PR	Peng-Robinson cubic EoS
RG	Real Gas
SNG	Synthetic Natural Gas
SRK	Soave-Redlich-Kwong cubic EoS
TCD	Thermal Conductivity Detector
UMR	Universal Mixing Rule
VLE	Vapor Liquid Equilibrium
VPL	Vapor-Pressure-Liquid

1. Introduction

Natural gas is a hydrocarbon mixture consisting primarily of methane CH_4 (70-90% v/v) and other hydrocarbon such as ethane, propane and butane. Non-hydrocarbon impurities such as H_2O, CO_2, N_2, H_2S can also be found in small amounts. Natural gas is the cleanest fossil fuel and can be used everywhere, from households to energy high-demanding industries. This is the reason why natural gas pipeline networks have been developed for the transportation of the gas throughout the world [1].

The knowledge of the hydrocarbon dew point (HCDP) is of great importance for the oil and gas industry. Natural gas pipelines are designed for single-phase transportation and, therefore, hydrocarbon condensation could have severe consequences for the safe transportation of the gas. In order to assure an effective utilization of the natural gas pipelines, accurate measurement and prediction of hydrocarbon dew points is necessary [2].

At the laboratory facilities of Statoil in Trondheim, an apparatus for measuring hydrocarbon dew points, named GERG rig, is available. The objective of this diploma thesis is the study of various factors affecting the accuracy of the hydrocarbon dew points and, therefore, the qualification of GERG rig for future measurements.

Adsorption phenomena are a known challenge in dew point measurements and have been studied in order to determine their effect on the measured dew points [2]. This study, which was performed using another dew point rig, in the frame of a master thesis also, showed the presence of adsorption and suggested the building of a dew point rig with less adsorbing material (GERG rig). Adsorption of the heavy compounds of the mixture leads to a change of the composition of the gas and, therefore, inaccurate measurements. The presence of adsorption inside GERG rig is investigated through the study of the parameters affecting the accuracy of the measured dew points.

Hydrocarbon dew point measurements have been conducted for two synthetic natural gases and one real. The first synthetic gas is a binary mixture of methane and n-heptane whereas the second consists of nitrogen, carbon dioxide and hydrocarbons from methane up to n-octane. The real gas is actually a rich gas that contains nitrogen and carbon dioxide as well as hydrocarbons up to n-decane.

In the oil and gas industry, thermodynamic models are used for the prediction of the phase envelope. Such models are both traditional cubic equations of state (EoS) and more advanced models. To evaluate the accuracy of these models, experimental data are required. In this work, the measured hydrocarbon dew points are used to evaluate three models: SRK [3] and PC-SAFT [4] equations of state as well as the UMR-PRU [5] model that belong to the class of the so-called EoS/G^E models.

In order to study the effect of the adsorption phenomena on the dew point measurements various operational parameters of the rig, related to adsorption, were examined. The parameters examined are:

- the volume of the gas used for each measurement,
- the temperature applied inside the chamber of the rig and
- the gas sample conditioning.

First, the theoretical background regarding the phase envelopes and the methods of measuring and determining the HCDP will be presented. Chapter 3 consists of the experimental work performed. The dew point measurements will be presented and discussed. The results from modelling work together with an uncertainty analysis are presented in Chapter 4. Finally, some concluding remarks and proposals for future work will be given.

2. Theoretical Background

This chapter present the theoretical basis required for the study of natural gas' thermodynamic behavior and its depiction on phase envelopes. In addition, a brief overview of the methods used in order to measure or determine the dew point of multi-component systems, such as natural gas, is performed, emphasizing to the methods being used in this work. Adsorption is a known challenge in dew point measurements and, therefore, adsorption theory is also presented.

2.1. Phase Envelope – HCDP

The thermodynamic behavior of natural gas is depicted on phase envelopes. A phase envelope indicates the thermodynamic behavior of a multi-component system, such as natural gas, and the conditions (pressure and temperature) where the different phases of the mixture occur [7]. A typical phase envelope of natural gas is presented on Figure 2.1.

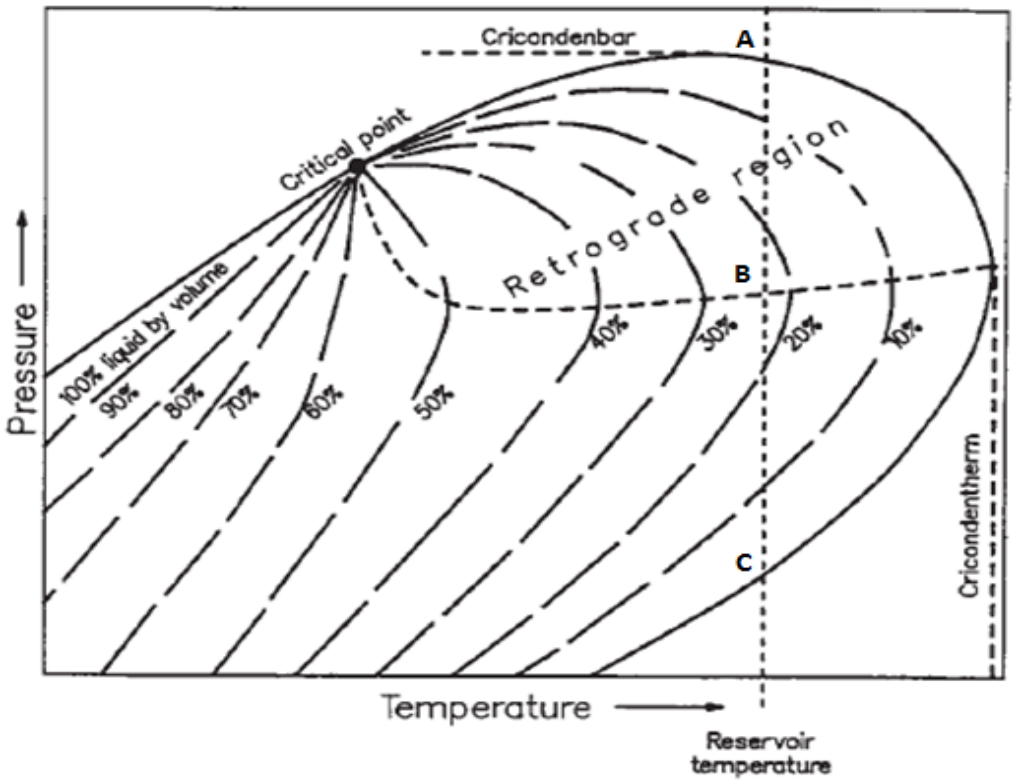

Figure 2.1: P-T diagram for a typical natural gas

The critical point for a multi-component system is the common point between the bubble point curve (the line of saturated liquid-100% liquid with a trace of vapor, on the left of the critical point) and the dew point curve (the line of saturated vapor-100% vapor with a trace of liquid, on the right of the critical point). It is the point for which liquid and vapor phases are indistinguishable. Outside the curve, there is a single-phase behavior: a liquid phase above the bubble point curve, a vapor phase above the dew point curve and a dense phase above critical point. [7]

Inside the curves, there is a two-phase region. The highest temperature and pressure at which liquid and vapor coexist are called cricondentherm (CCT) and cricondenbar (CCB) respectively [7]. The knowledge of the CCT and CCB and the dew point curve is crucial for the natural gas' safe transportation. The hydrocarbon dew point is universally used in the natural gas industry as an important quality parameter, stipulated in contractual specifications and enforced throughout the natural gas supply chain, from producers through processing, transmission and distribution companies to final end users [6].

The two-phase region to the right of the critical point is called retrograde region as a different behavior of the mixture is met. Inside the curve, each one of the existing lines represents a stable percentage of the liquid phase by volume. The critical point is the boundary of the two phases where their thermodynamic properties are the same. Consider we are in the vapor phase and in a temperature greater than the critical and lower than the cricondentherm. As we are entering the two-phase region, with a pressure decrease, we will start to produce some liquid. But, there will be a point (of maximum liquid quota) where that liquid will start to vaporize. In other words, even though we are compressing the system, liquid will vaporize and not condense. The dotted line AB in Figure 1 inside the retrograde region indicates the maximum volume ratio liquid/vapor met at a specific temperature. As the pressure drops the mixture becomes richer in liquid phase until the horizontal dotted line – from then on, the vapor phase becomes richer until 100% vapor is reached [7].

Figure 2.2 illustrates a typical vapor-pressure-liquid (VPL) diagram for multi-component mixtures which shows how the liquid volume of the mixture changes with pressure. As it can be noticed, for an isothermal increase of the pressure, the percentage of the liquid phase increases until a maximum quota. From then on, the liquid that has been formed starts to vaporize, thus the curve declines.

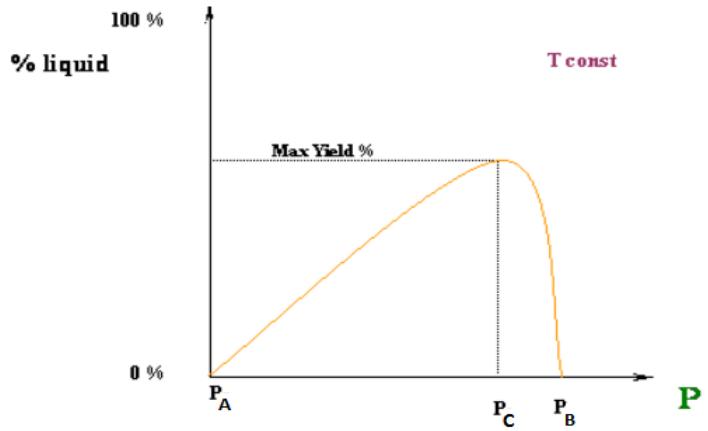

Figure 2.2: VPL diagram for condensate region

The shape of the phase envelope is defined by the *composition* of the mixture as it is the one that defines its thermodynamic behavior. In order to study the effect of the composition on phase envelopes, the composition of natural gas is theoretically divided into two main categories: the light fraction (methane to hexane) and the heptanes plus (C7+) fraction (heavy). Certainly, the non-hydrocarbons (carbon dioxide, nitrogen etc) form another fraction [9]. The C7+ fraction is very important for the dew point measurements since they are the heavy hydrocarbons that are adsorbed inside the dew point apparatus.

The heptanes plus fraction is used to simplify the composition of natural gas in case there is significant number of heavy components. The characterization of C7+ fraction is essential when using equations of state. According to the properties of all the heavy components as a whole, usually several heptane plus components are used, called pseudo-components to best describe the behavior of the C7+ fraction [10].

The amount and properties of the C7+ fraction has significant effect on the phase envelope of natural gas and especially in the dew point line. By using Peng-Robinson Equation of state [11], the impact of the C7+ fraction on the phase envelope of natural gas has been studied. The composition of the natural gas used for characterization in this case is shown in Table 2.1.

Table 2.1: Composition of natural gas used to study the effect of C7+ fraction

Component	mol
Methane	0.7252
Ethane	0.1584
Propane	0.0751
i-butane	0.0094
n-butane	0.0202
i-pentane	0.0034
n-pentane	0.0027
n-hexane	0.0028
C_{7+} fraction	0.0030

Figure 2.3 shows the calculated with PR EoS phase envelopes for different characterizations of C7+ fraction. It is noticed that as the molecular weight of the C7+ fraction increases, the shape of the phase envelope extends. Specifically, the critical point moves slightly to the left while the cricondenbar and cricondentherm increases.

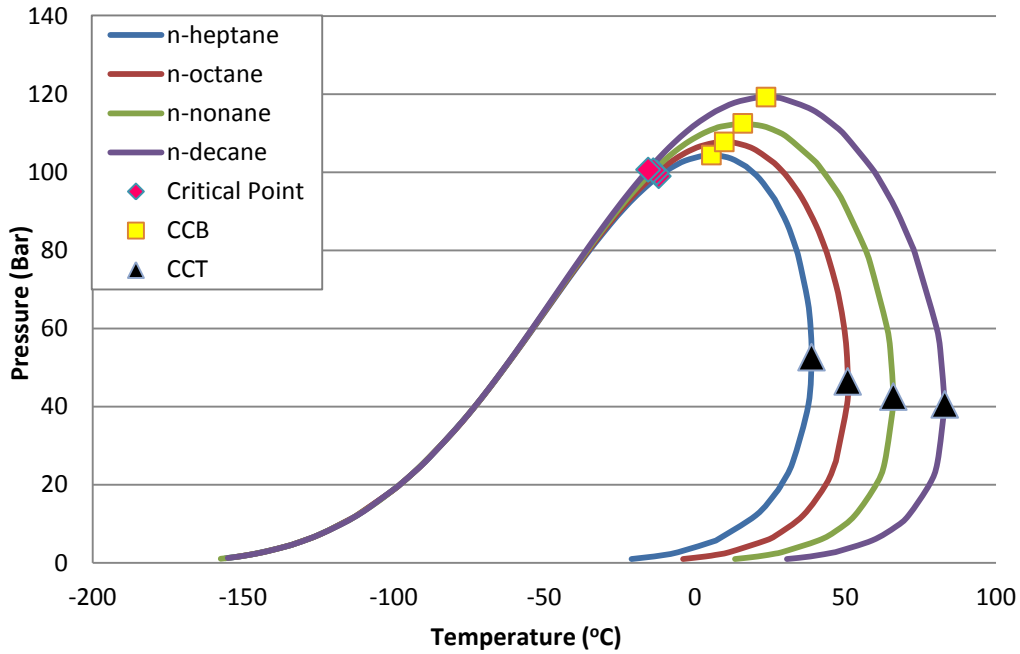

Figure 2.3: Impact of C7+ fraction on natural gas phase envelope

By selecting the n-heptane as the C7+ fraction, the impact of different mole fractions has been studied as it is illustrated in Figure 2.4. Increase of the composition of the heptane in the mixture, leads to movement of the critical point to the right and increase of CCB and CCT.

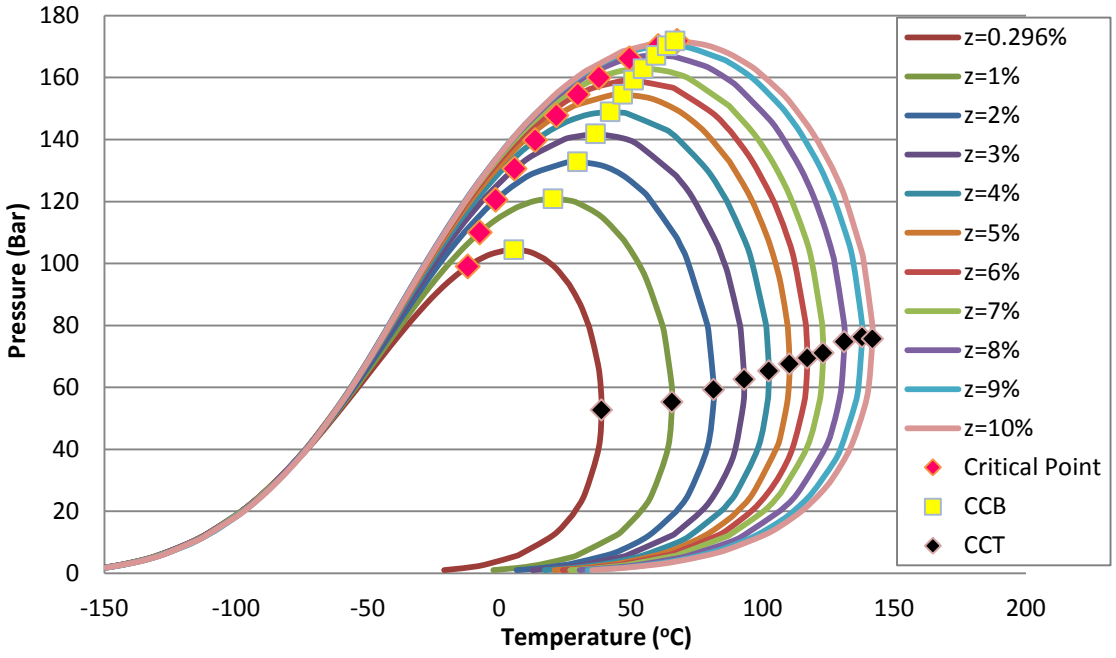

Figure 2.4: Impact of different mole fractions of heptane on natural gas phase envelope

It is worth mentioning that in higher concentrations, an increase of 1% in heptane's mole fraction, e.g. from 9% to 10%, result in a smaller increase of CCB and CCT than in lower concentrations, e.g. from 1% to 2%.

In conclusion, the heavier the compound and the higher the concentration of the heavy component, the wider the phase envelope is. In case when adsorption takes place, the concentration of the heaviest compounds will be lower, thus, the dew point measured will be lower than the actual one.

2.2. Direct Methods of measuring HCDP

Direct methods of measuring HCDP are in fact experimental methods. There are two different categories for direct measurement of hydrocarbon dew points; manual and automatic visual dew point methods [12]. In this work, hydrocarbon dew points of natural gas are measured using the manual visual dew point method.

2.2.1. Manual visual dew point method

The manual visual dew point method is the simplest and most widely used method for measuring HCDP. Manual systems, such as the Bureau of Mines dew point meter, regard the HCDP as the temperature at which hydrocarbon condensates first begin to form a visible deposit on a surface, when the gas is cooled at a constant pressure [13]. The device used at this method consists of a mirror that separates two chambers; the sample chamber where the sample gas flows and the chamber where a coolant flows decreasing the temperature of the mirror. An operator manually cools the mirror until the onset of condensation can visually be detected. The formation of the dew is observed as a very small droplet or even a mist on the mirror [8].

According to the experience of the operator, it is possible to detect, besides hydrocarbon dew points, also water dew points and a contaminated dew point. The method requires a lot of training and patience for the operator to be able to see the dew and control the cooling rate of the mirror. Given that the condensates require some time to be visible on the mirror, slow cooling is necessary. Because the dew point is observed by the human eye, the method is subjective [8].

2.2.2. Automatic optical condensation method

The method of automatic optical condensation is a fully automated process that does not require an operator to see the formation of dew. It is based on the same principle as the manual visual method (isobaric cooling) but differs from it in many aspects. First, repeatable measurements are conducted providing the user with up to six measurement cycles per hour. It consists of a light source, a detector and an optical surface on which the detection of the dew is performed. As the temperature on the surface decreases, a layer of condensates is formed. The light aiming to the surface is then diffused and, according to the intensity of the scattered light, the detector records the hydrocarbon dew point. Furthermore, in order to avoid accumulation of heavy

hydrocarbons caused by a continuous flow of gas, the amount of the gas measured is specified and trapped in the measuring chamber [8].

Automatic systems' main advantage over manual visual dew point method is that it is an objective method. In addition, neither training nor specific skills are required to operate such device. The operator's error is eliminated whereas the repeated measurements lead to more accurate dew points. The weakness of this method over the manual method consists of its limitation to accurately measure the HCDP if water or glycol traces are present on the sample [8].

2.3. Indirect Methods of HCDP determination

The most common indirect method uses a combination of gas chromatography (GC) to determine the composition of the gas mixture and a thermodynamic model in order to calculate the dew point curve of the gas. The accuracy of such method depends both on the accuracy of the GC and the successful phase envelope prediction of the model used. Indirect methods have an advantage over direct methods as the determination of the hydrocarbon dew point is possible at any pressure.

2.3.1. Gas Chromatographic Analysis

Gas chromatographic analysis is the first part of the indirect method of determining HCDP. The final composition that is given as input in the second part of this method, the thermodynamic models, requires the application of a characterization method. Thus, the characterization method used in this work is also presented below.

2.3.1.1. Principles of gas Chromatography

Gas chromatography (GC) is defined as the group of analytical separation techniques used to analyze volatile substances in the gas phase. In gas chromatography, the components of a sample are dissolved in a solvent and vaporized in order to separate the analytes by distributing the sample between two phases: a stationary phase and a mobile phase. The stationary phase is either a solid adsorbent (gas-solid chromatography-GSC) or a microscopic layer of liquid or polymer on an inert solid support (gas-liquid chromatography-GLC). The stationary phase is inside a piece of glass or metal tubing called a column. The mobile phase is a chemically inert gas that serves to carry the molecules of the analyte through the heated column, such as helium and nitrogen. Gas chromatography is one of the sole forms of chromatography that does not utilize the mobile phase for interacting with the analyte [14].

The instrument used to perform gas chromatography is called a gas chromatograph. The gas is injected in the head of the column through a sample port. Usually, three repeated injections are performed. There are two types of GC columns: packed and

capillary. Packed columns are typically a glass or stainless steel coil that is filled with the stationary phase and capillary columns are a thin fused-silica capillary that has the stationary phase coated on the inner surface. Capillary columns provide higher separation efficiency than packed columns [14].

The device that provides the user with the quantitative measurement of the components of the mixture as they elute in combination with the carrier gas is called detector. There are different types of detector such as flame ionization detectors (FID), thermal conductivity detectors (TCD), electron-capture (ECD) etc. FID and TCD detectors are the most commonly used; FID measures the organic species in the gas stream with high accuracy and TCD is able to detect the changes in thermal conductivity, and hence, distinguish all components but with low accuracy [10]. The combination of detectors is essential in order to obtain as high accuracy as possible in the measurements [14].

Gas chromatography is widely preferred because of it is a highly sensitive and fast method. Volatilization of the mixture is the only limitation of this technique, which is not a real issue in the natural gas industry, where the samples are already in the gas phase [14].

2.3.1.2. Characterization of C7+ fraction

The composition deriving from the GC analysis is then used as an input for thermodynamic models to predict the dew point curve of the sample gas. These models require information such as the critical properties, acentric factor, molecular weight, binary-interaction parameters of all components in a mixture. Nowadays, the existing chemical-separation techniques are not adequate for the identification of all hundreds of components found in reservoir fluids. This is the reason why a characterization of the heavy hydrocarbons of a mixture using experimental and mathematical methods is established [9].

The method used in this work characterizes the C7+ fraction by employing a PNA distribution. In this distribution the aim is to put all components with boiling points within a specific range into a selected Paraffin (e.g. n-heptane for C7), Naphtene (e.g. cyclo-hexane for C7) or Aromate (e.g. benzene for C7).

The variation employed in this diploma thesis is that, methyl cyclohexane is used to represent the naphthenic part of C8 fraction instead of cyclo-heptane and ethyl-cyclohexane instead of cyclo-octane [9].

2.3.2. Thermodynamic models

The application of thermodynamic models in dew point prediction is the second part of an indirect hydrocarbon dew point determination. Three models are employed in this work: SRK and PC-SAFT equations of state and, the UMR-PRU model.

2.3.2.1. SRK

The SRK equation [3], is one of the first and most important modifications on the Van der Waals EoS [13], and is expressed as follows:

$$P = \frac{RT}{V-b} - \frac{a}{V(V+b)} \tag{2.1}$$

where P is the pressure, T is the temperature, V is the volume and R is the gas constant.

The attractive and repulsive parameters, a and b, for pure components are given by:

$$a = 0.42748 \frac{(RT_c)^2}{P_c} a(T) \tag{2.2}$$

$$b = 0.08664 \frac{RT}{P_c} \tag{2.3}$$

$$a(T) = \left[1 + m\left(1 - T_r^{0.5}\right)\right]^2 \tag{2.4}$$

$$m = 0.48508 + 1.55171 \cdot \omega - 0.15613 \cdot \omega^2 \tag{2.5}$$

The numerical values in Eq. (2.2), (2.3) and (2.5) were suggested by Grabowski and Daubert [14].

The reduced temperature T_r is given by:

$$T_r = \frac{T}{T_c} \tag{2.6}$$

2.3.2.2. PC-SAFT

The PC-SAFT EoS [4] is based on the SAFT EoS [17-18], but a new dispersion term is included which explicitly accounts for the chain-length dependencies of the interactions. Thus, for non-associating compounds, the compressibility factor is calculated as the sum of the ideal gas contribution ($Z^{id} = 1$), a hard-chain contribution (hc), and a perturbation contribution, which accounts for the attractive interactions (disp).

$$Z = Z^{id} + Z^{hc} + Z^{disp} \tag{2.7}$$

where Z is the compressibility factor, with $Z = Pv/(RT)$, P is the pressure, v is the molar volume and R is the gas constant. The hard chain contribution (*hc*) is given by

$$Z^{hc} = \bar{m} Z^{hs} - \sum_i x_i (m_i - 1) \rho \frac{\partial \ln g_{ii}^{hs}}{\partial \rho} \tag{2.8}$$

$$\bar{m} = \sum_i x_i m_i \tag{2.9}$$

where x_i is the mole fraction of chains of component i, m_i is the number of segments in a chain of component i, ρ is the total number density of molecules, g_{ii}^{hs} is the radial pair distribution function for segments of component i in the hard sphere system, and the superscript *hs* indicates quantities of the hard-sphere system.

The parameters for a pair of unlike segments are obtained by the conventional Berthelot-Lorentz combining rules:

$$\sigma_{ij} = 1/2 \cdot (\sigma_i + \sigma_j) \tag{2.10}$$

$$\varepsilon_{ij} = \sqrt{\varepsilon_i \varepsilon_j} (1 - k_{ij}) \tag{2.11}$$

where the binary interaction parameter, k_{ij}, is introduced to correct the segment-segment interactions of unlike chains.

2.3.2.3. UMR-PRU

UMR-PRU model is a predictive EoS that belongs to the class of the so-called EoS/G^E models. It combines the PR EoS with an original UNIFAC-type G^E model [19].

The PR EoS, introduced in 1976 by Peng and Robinson [11], in order to improve the liquid density predictions, is another variation of the van der Waals EoS:

$$P = \frac{RT}{V-b} - \frac{a}{V(V+b)+b(V-b)} \qquad (2.12)$$

where a is also expressed by Eq. (2.4) with

$$m = 0.37464 + 1.54226 \cdot \omega - 0.26992 \cdot \omega^2 \qquad (2.13)$$

and

$$b = 0.0778 \frac{RT_c}{P_c} \qquad (2.14)$$

The original UNIFAC-type G^E model employs temperature dependent group-interaction parameters, through the Universal Mixing Rules (UMR) proposed by Voutsas et al. [20]:

$$\frac{a}{bRT} = \frac{1}{A}\frac{G_{AC}^{E,SG} + G_{AC}^{E,res}}{RT} + \sum_i x_i \frac{a_i}{b_i RT} \qquad (2.15)$$

and

$$b = \sum_i \sum_j x_i x_j b_{ij}, \qquad b_{ij} = \left(\frac{b_i^{1/2} + b_j^{1/2}}{2} \right)^2 \qquad (2.16)$$

The parameter A (Eq. 2.15) is equal to -0.53 for the PR EoS, while $G_{AC}^{E,SG}$ and $G_{AC}^{E,res}$ are the Staverman-Guggenheim term of the combinatorial part and the residual part of the excess Gibbs energy (G^E) respectively, which are calculated from UNIFAC through the following equations:

$$\frac{G_{AC}^{E,SG}}{RT} = 5 \sum_i x_i q_i \ln \frac{\theta_i}{\phi_i}, \qquad \frac{G_{AC}^{E,res}}{RT} = \sum_i x_i \nu_k^i \left(\ln \Gamma_k - \ln \Gamma_k^i \right) \qquad (2.17)$$

$$\ln \Gamma_k = Q_k \left[1 - \ln\left(\sum_m \theta_m \Psi_{mk} \right) - \sum_m \frac{\theta_m \Psi_{mk}}{\sum_n \theta_n \Psi_{nm}} \right] \qquad (2.18)$$

For compound i: $$\phi_i = \frac{x_i r_i}{\sum_j x_j r_j}, \qquad \theta_i = \frac{x_i q_i}{\sum_j x_j q_j} \qquad (2.19)$$

For group m: $$\theta_m = \frac{Q_m X_m}{\sum_n Q_n X_n}, \qquad X_m = \frac{\sum_j \nu_m^{(j)} x_j}{\sum_j \sum_n \nu_n^{(j)} x_j} \qquad (2.20)$$

The parameter Ψ in the residual part is a function of the group interaction parameters (IPs), which are taken from the UNIFAC proposed by Hansen et al. [19], except from the pairs that contain gases which are determined by fitting binary VLE data. Since the VLE binary systems that contain gases cover a large temperature range, the Ψ function adopted is the following:

$$\Psi_{nm} = \exp\left[-\frac{A_{nm} + B_{nm} \cdot (T - 298.15) + C_{nm} \cdot (T - 298.15)^2}{T} \right] \qquad (2.21)$$

3. Experimental Work

The aim of this chapter is to present the experimental work performed in this study. It consists of the description of the HCDP experimental apparatus and procedure, the calibration of the instruments used and the HCDP measurements. Both a pure component and natural gases were measured.

The natural gases used in this work are two synthetic and one real gas. Various parameters affecting the HCDP measurements were studied:

- the volume of the sample measured, which will be referred to as ***volume effect***
- the temperature of the chamber where the dew point measurements take place, which will be referred to as ***temperature effect***, and
- The preheating of the bottle or cylinder that contained the gas, which will be referred to as ***sample conditioning effect***.

The repeatability of the dew points measurements was also studied. The various effects are discussed and, finally, conclusions are drawn based on the effect observed.

3.1. Dew Point Measurements

A good understanding of the hydrocarbon dew point measurements requires the knowledge of the principles governing these measurements. The experimental apparatus and procedure are presented below. Furthermore, the challenges faced and the modifications conducted in the frame of this diploma thesis follow.

3.1.1. Principle of dew point measurements

Isobaric cooling is the principle on which dew point measurements are based. Prerequisite for an accurate dew point measurement is the maintenance of the sample gas in single-phase region. The dew point observation is the result of a gradual decrease of temperature at constant pressure. In other words, for every pressure level the operator is interested in, the temperature is being decreased slowly until the detection of the dew. Figure 3.1 is representative of the dew point measurement principle.

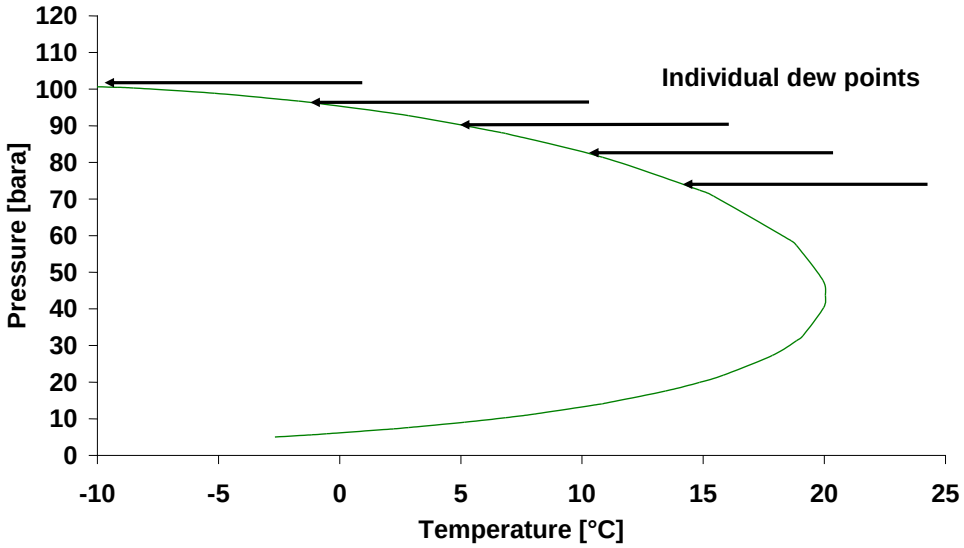

Figure 3.1: Isobaric cooling

Assume that the operator is interested in measuring the hydrocarbon dew point of a sample at constant pressure that the gas is in single-phase region (end of the arrows). The operator is decreasing slowly the temperature until the first dew begins to form. The dew is formed when the dew point curve is reached (tip of the arrows). This is the HCDP of the gas being measured for the specific pressure. The temperature then increases so as the gas moves outside the two-phase region.

3.1.2. Experimental equipment

- Dew point Apparatus

The experimental equipment used is a custom made apparatus for measurement of hydrocarbon dew points for natural gases. The rig has been built up in the Statoil R&D laboratories in the frame of a previous project and it has been named after it; GERG rig (Figure 3.2).

Figure 3.2: Front (left) and back side (right) of the experimental apparatus

The experimental apparatus consists of two pistons circulating the sample gas in a gas flow loop. The pistons, having 1 lt volume each, are used for both circulation of the gas and adjustment of the pressure level. The gas is circulated clockwise through a specific valve arrangement (EV-1, EV-4 and EV-2, EV-3 open/close in pairs). The gas is inserted inside the loop through a regulating valve and is circulated according to the Process Flow Diagram (Figure 3.3). The filling pressure of each experiment varies, depending on the pressure of the natural gas sample. All piping of the gas flow loop is micro polished in order to minimize adsorption phenomena.

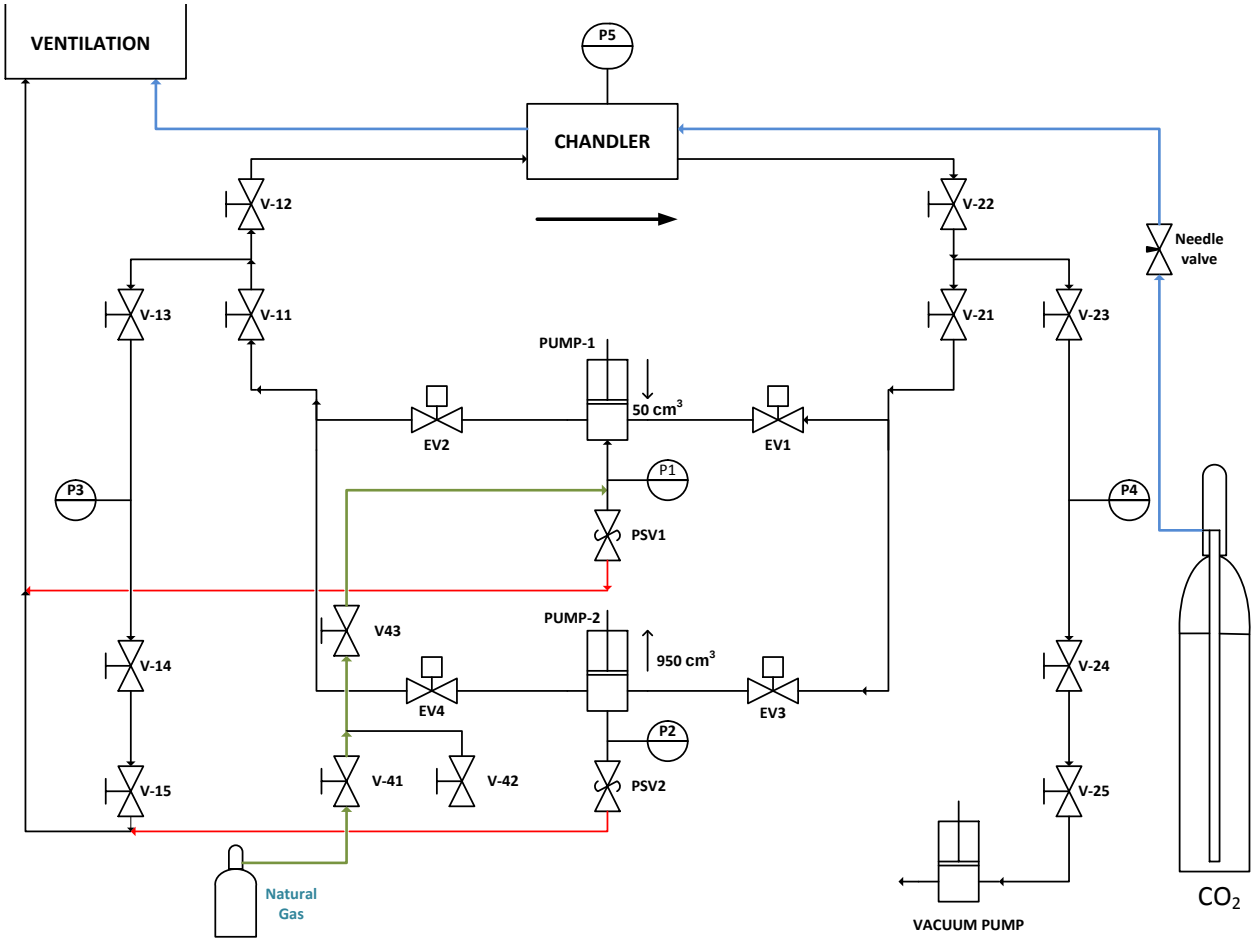

Figure 3.3: Process Flow Diagram of experimental apparatus

As the gas is circulated in a closed loop, it passes in front of a mirror whose temperature is controlled by fitting a cooled copper rod to the back of it. Liquid carbon dioxide is used to cool the copper rod, and therefore indirectly the mirror, through a hand-regulated valve. This cooling system allows dew point detection down to -40 ^{o}C. The dew point mirror and cooling system are manufactured by Chandler Engineering (**Figure** 3.4)

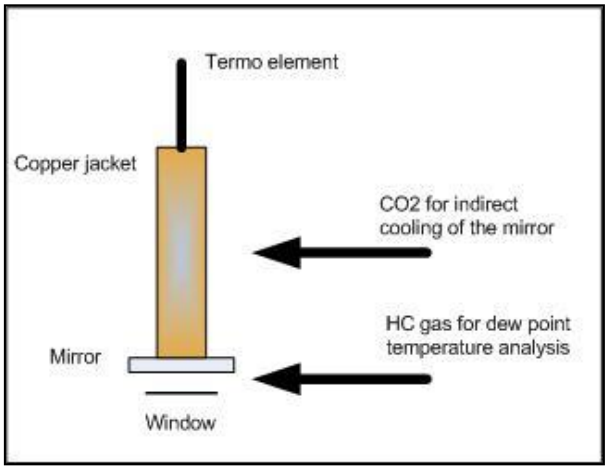

Figure 3.4: Schematic sketch over the cooling system

The temperature of the mirror is measured by a Pt-100 element in direct contact with the back of the mirror. The thermo element is connected to a Dostmann P655-EX thermometer which displays the temperature indication. The uncertainty of the thermometer is ±0.1°C in the region -100°C to 150°C.

All external piping is heat traced to a temperature of 60°C to prevent effects of condensation and adsorption during filling of the gas. The temperature of all parts of the experimental apparatus is controlled by placing it in a temperature controlled chamber. The heating control system, West P600 Process Controller, presents an accuracy of 0.1% of input range. Temperature safety barriers accompany all the heating elements.

The measurements can be conducted up to 200 bar. Four Keller 33X-Ei pressure transmitters of 0.1% accuracy are used as indicated in Figure (PFD). Two pressure safety valves (PSV) ensure maximum pressure of 200 bar. The rig' pressure is controlled by a computer program according to the values of manometers P1 and P2. Besides pressure, circulation and flow of the gas are also controlled through the computer program.

- Gas Chromatograph

As far as the GC analysis is concerned, an HP 6890 Series gas chromatograph from Agilent Technology, where hydrocarbons from C1 to C15 are separated on a HP-PONA capillary column (50mx200 micron, 0.5 micron film thickness) and a flame detector (FID). Separation of oxygen / argon, nitrogen, carbon dioxide, methane, ethane and propane are done in a PoraPlot Q-HT capillary column (25x320micron, 20 micron film thickness) and a Molsieve 5Å capillary column (10mx320 micron, 20 micron film thickness) with detection on a thermal conductivity detector (TCD).

3.1.3. Experimental Procedure

The day before the experiment is carried out, the experimental apparatus and all external piping are put in vacuum at a controlled temperature of 60°C for at least 12 h over the night. During the preparation of the apparatus, before vacuumization starts, heat conducting paste to enhance the heat flow is put on the temperature element and the mirror is carefully cleaned. Then, the system is filled with the desired volume of gas sample to the highest possible pressure. Pressure is checked in order to detect leakage if any. The temperature in the chamber is set to the desired value.

After filling the rig, the gas is circulated for 20 min at 2000cc/h to eliminate composition gradients inside the rig and evaporate gas that may have condensed during filing. The pressure level at which the dew point measurements will be performed is then set and the gas is circulated for 10 min for the system to be stabilized. Such circulation of the gas is performed every time the pressure of the dew point measurement is changed. The mirror is cooled slowly with a typical rate of 1.5°C/min while the gas is circulated at 400cc/h until the dew is detected (T_{cool}). The dew appears as a light grey to grey circle in the middle of the mirror and is increases in size as the temperature decreases. The minimum temperature achieved (T_{min}) must not differentiate more than 1°C from the temperature at which it is detected. As soon as the dew is observed on cooling, the mirror is heated for the hydrocarbons to evaporate (T_{heat}). The formation of the dew requires some amount of gas to condense and some time to be noticeable. Thus, the dew point temperature is estimated as the average of the first point of visuable condensation and the point of total evaporation. The difference in temperature where the dew is first formed and to that of total evaporation must be less than 0.5°C. Three parallel measurements are required. The average of the three measurements is considered the dew point.

The detailed experimental procedure can be found in Appendix A.

3.1.4. Challenges with experimental work

- Adsorption

The main challenge of the hydrocarbon dew point measurements is the presence of adsorption phenomena. Adsorption is defined as the adhesion of particles from a gas, liquid, or dissolved solid to a surface; the opposite process is desorption. Adsorption is affected by many factors such as temperature, pressure and the surface material.

Adsorption phenomenon is described by Langmuir isotherm equation:

$$\theta = \frac{KP}{1 + KP} \qquad (3.1)$$

where θ is the surface coverage given as the fraction of adsorption sites occupied, K is the equilibrium constant and P is the pressure.

This means that the higher the pressure is, the more θ approaches unity, therefore, full surface coverage.

Moreover, adsorption is an exothermal reaction while desorption is an endothermal one. Thus, at constant pressure, high temperature promotes desorption.

Inside the dew point apparatus, gas particles are often adsorbed onto the surface of the rig resulting into a change to the composition of the gas. The components adsorbed are the heavier compounds of the mixture which are mostly responsible for the shape of the dew point line. When heavy components are adsorbed, the sample gas becomes lighter and, therefore, the dew point line moves to the left. As a result, the dew point is measured at a lower temperature. The measurements are, therefore, inaccurate and the experimental dew points are not representative of the sample gas.

The study of volume effect, chamber's temperature effect and sample conditioning effect derive from the need to ascertain the existence or not of adsorption phenomena inside GERG rig.

- Maintain the gas sample in the single phase

Essential for the HCDP measurement is also to maintain the sample gas in the single-phase region during the preparation and the filling of the rig. Otherwise, heavy components' condensation will result in change of the composition. Single-phase gas sample must be, firstly, ensured inside the sample cylinder. If the phase of the gas is in doubt, the sample must be heated, so as to evaporate any in the bottle. Another way to avoid a two-phase sample in the bottle is to pressurize it with argon. Secondly, risk of condensation exists during filling due to the Joule-Thomson effect. This is the reason why slow filling and heating of all external piping is necessary.

- Dew Point detection

The detection of the dew is also to be considered. While performing the dew point measurements, it was noticed that, at high pressures, the dew formation is difficult to be seen.

- Manual CO_2-cooling

Furthermore, while cooling the chilled mirror, sudden expansion of liquefied carbon dioxide in high pressure to atmospheric pressure leads to the formation of dry ice inside the CO_2 piping. Clogging of the piping makes it difficult to perform the dew point measurements in two ways. First, if the dew has not been formed yet, the dew point temperature cannot be reached. Secondly, if the dew has already been detected, unclogging of the piping while temperature increases and condensates on the mirror evaporate, leads to excessive flow of the trapped CO_2 and, therefore, the subcooling destroys the measurement.

3.1.5. Modifications/Improvements/Maintenance

Prior to any experimental measurements were performed, several modifications had to be done to the GERG rig. Some of them concerned maintenance issues such as pressure test of the pressure safety valves and change of the lubrication oil from the

pumps, while others were necessary for the good performance of the apparatus. For instance, the heating control system needed to be installed and the proper functioning of the heating jacket needed to be tested. In addition, a heat trace in the gas line was put and tested in order to avoid condensation of the heavy hydrocarbons during filling.

Furthermore, during the experiments, new needs were identified in order to improve the rig's functionality or deal with raised difficulties. Replacement of the CO_2 and the gas line to more flexible ones, change of CO_2 piping in order to avoid the formation of dry ice, installation of a noise reduction system and stabilization and repair of the ventilation hose are some of the required actions.

3.2. Pressure and temperature calibration

Calibration was required before conducting the dew point experiments in order to ensure maximum accuracy of the pressure and temperature measurements in the rig.

Pressure calibration

Due to the complicated software used by GERG rig, it was decided to calibrate the rig as a whole. The pressure transmitter of high accuracy and the specially made for pressure calibration set-up used are shown at Figures 3.5 to 3.6. Nitrogen was used as calibration gas.

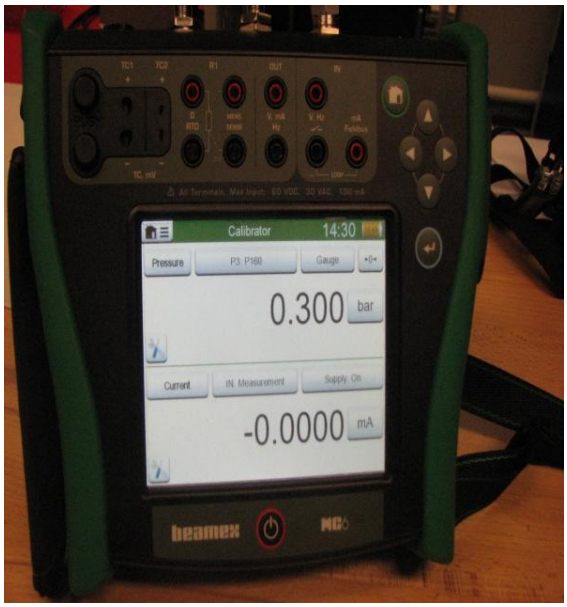

Figure 3.5: High accuracy pressure transmitter

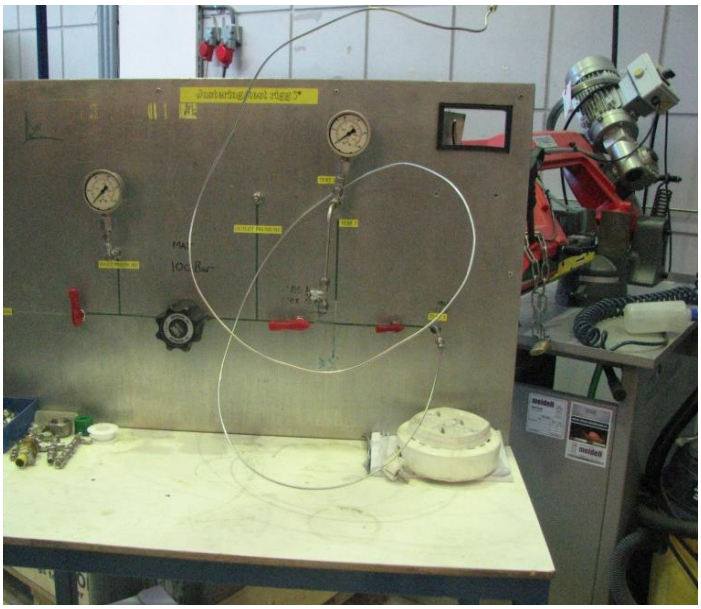

Figure 3.6: Pressure calibration set-up

The need for pressure calibration is better illustrated in Table 3.1.

Table 3.1: Typical pressure indications of the manometers used under vacuum

Manometer	Pressure (bar)
P1	0.30
P2	-0.06
P3	0.00
P4	0.17

The calibration pressures and the manometers' indications respectively are shown in Table 2. The range in which the manometers were calibrated is the range of measuring pressures, 5 – 120 bar approximately.

Table 3.2: Calibration pressures and manometers' indications in bar

P_{cal}	$P1_{read}$	$P2_{read}$	$P3_{read}$	$P4_{read}$
6.54	6.61	6.54	6.36	6.47
22.62	22.72	22.62	22.48	22.58
52.22	52.25	52.19	52.10	52.17
81.10	81.19	81.13	81.08	81.13
101.69	101.76	101.71	101.69	101.72
127.27	127.35	127.30	127.32	127.34

All manometers show accuracy within 0.1 bar except for P3 that presents a deviation of 0.2 bar (Deviations can be found in Appendix B, Tables B.1 to B.4). The measurements are not in accordance with the technical data for the dew point rig which indicate accuracy in pressure stability of 0.05 bar. However, deviations up to 0.2 bar are considered adequate and, therefore, the pressure accuracy is considered as 0.2 bar for this work. Either way, pressure stabilization inside GERG rig is based only on P1 and P2 indications.

Temperature calibration

Dostmann P 655-EX thermometer and Pt 100 thermo element were necessary to be calibrated as they are the dew point's temperature measuring instruments.

Calibration of this type of thermometers is actually a calibration in the probe of the apparatus. Therefore, the conclusion that will be drawn later on this subsection can safely be used only when the particular thermometer is accompanied with the thermo element with which it was calibrated and it is connected to the measuring port used during calibration (channel 1).

The range of measuring temperatures is approximately -40 to 20 °C. A glycol bath was used to calibrate the instruments down to -20 °C. Because the temperature indicator of the bath is not trustable, a reference thermo element, similar to the one used for the experiments, was also used for measuring the real temperature of the bath (Figure 3.7).

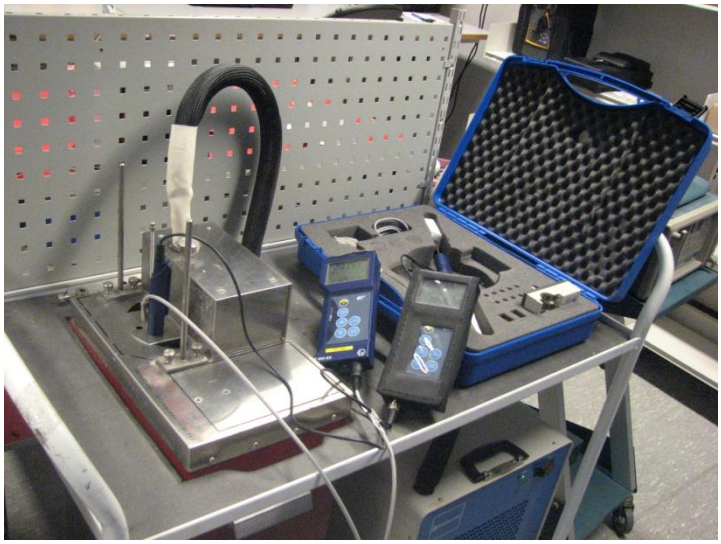

Figure 3.7: Temperature calibration device

The results of the calibration are shown in Table 3.3.

Table 3.3: Calibration temperatures and thermo element's indications in Celsius

T_{bath}	T_{cal}	T_{read}
-10	-8.38	-8.57
-5	-4.41	-4.58
0	0.12	0.02
5	5.05	4.93
10	9.92	9.86

It is obvious that the calibration values and the measured ones are similar presenting deviations up to 0.2 °C. The measurements are not in accordance with the technical data for P 655-EX thermometer which indicate an accuracy of ±0.1 °C in the range from -100 °C to +150 °C. However, the thermometer is considered accurate and calibration is not required.

Despite the fact that the deviations are minor, a tendency to increase as temperature decreases is observed (see Appendix B, Table B.5). Since dew point measurements in this work were performed down to approximately -40°C, an error greater than 0.2 °C in temperature should be expected. Based on the tendency noticed, this deviation is not expected to surpass 0.5°C.

What is more, any doubts as far as the negligibility of the deviations is concerned, during both pressure and temperature calibrations, are vanished when one considers the always present observer's error.

3.3. Measurement of a pure component

In order to test the rig's ability to measure accurate dew points, a pure component is measured. Ethane measurements are conducted with and without heating inside the chamber so as to test the temperature effect in a pure component. In addition, the experimental data are compared with literature data obtained from NIST database [21]. Both literature and experimental data can be found in Appendix C, Table C.1.

The results for ethane are illustrated on **Figure 3.8**.

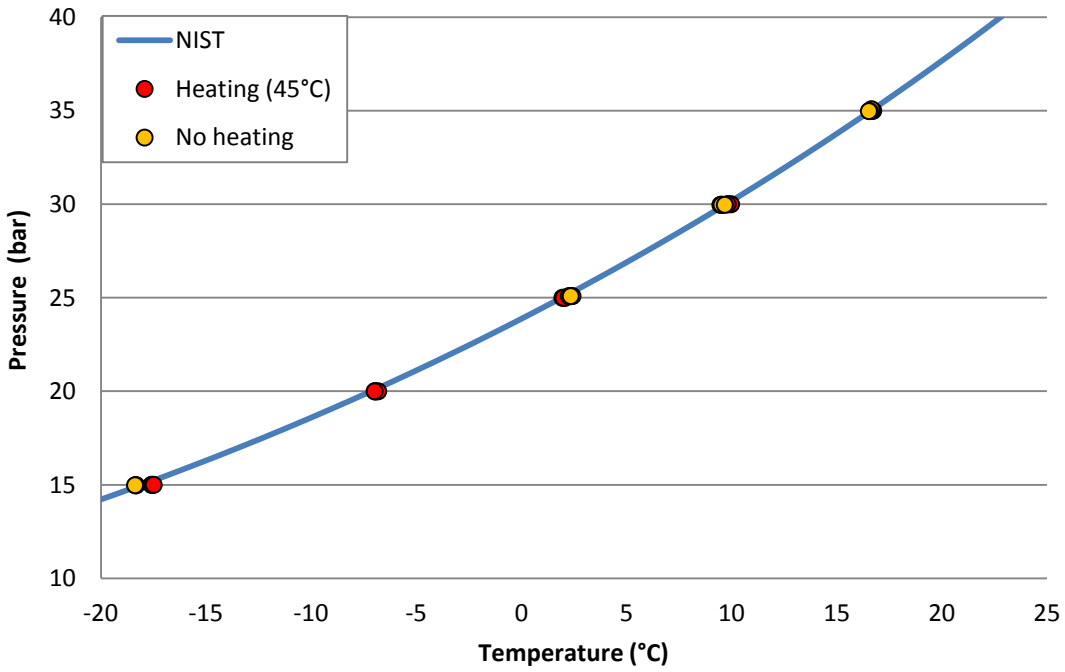

Figure 3.8: Experimental and literature data for ethane

The differences between the measured dew points with heating and literature data are presented in Table 3.4. It must be underlined that the temperature average of the three parallel dew points measurements, as described earlier (see subsection 3.1.3), is used in the estimation of the deviations.

Table 3.4: Deviations between literature and experimental data for ethane

	T_literature	T_exper.	
P (bar)	T (°C)	T (°C)	ΔT*
35	16.63	16.71	-0.08
30	9.74	9.89	-0.15
25	1.92	2.02	-0.10
20	-7.16	-6.92	-0.24
15	-18.07	-17.55	-0.52

*ΔT= T_literature - T_exper.

Based on the temperature accuracy indicated earlier (see. subsection 3.2), all deviations can be considered negligible apart from the deviation of 0.52 ^{o}C at 15 bar. In order to evaluate the importance of this deviation, the pressure deviation was studied as shown in Table 3.5.

Table 3.5: Deviations between literature and experimental saturation pressures for pure ethane

	P_exper.	P_literature	
T (°C)	P (bar)	P (bar)	ΔP*
16.71	35	35.05	0.05
9.89	30	30.11	0.11
2.02	25	25.05	0.05
-6.92	20	20.08	0.08
-17.55	15	15.20	0.20

*ΔP= P_literature - P_exper.

The maximum pressure which is indicated at 15 bar is 0.2 bar. This is the pressure accuracy as it was defined during pressure calibration. Thus, the difference noticed above is considered within experimental error.

3.4. Measurement of natural gas composition

Three natural gases were used on this work; two synthetic gases, SNG 2 and SNG 3, and one real gas, RG1. SNG 2 is a binary gas while SNG 3's composition is similar to a real gas' composition containing nitrogen, carbon dioxide and hydrocarbons up to n-octane. Both of them have also been used in previous work about adsorption on another dew point rig of Statoil [3]. The composition of RG1 is more complicated including also non-hydrocarbons as well as paraffinic, naphthenic and aromatic components up to n-decane.

A Gas Chromatograph was used to determine the composition of each gas. As far as the SNGs are concerned, the composition given from the manufacturer (Yara) was known. Due to the fact that these gases were ordered and delivered in 2010 and because experience has shown that the composition is changing during time, the need for a new composition analysis was raised. Both gases presented a change of composition compared to the one certified by Yara. UMR-PRU model was used to evaluate the significance of the composition differentiation observed.

– SNG 2

The difference in composition of SNG 2 seemed insignificant (Table 5).

Table 3.6: Composition of SNG 2

Yara GC analysis (2010)		*Statoil GC analysis (2013)*	
Component	**mol %**	**Component**	**mol %**
Methane	99.9	Methane	99.90955
n-Heptane	0.1	n-Heptane	0.09045

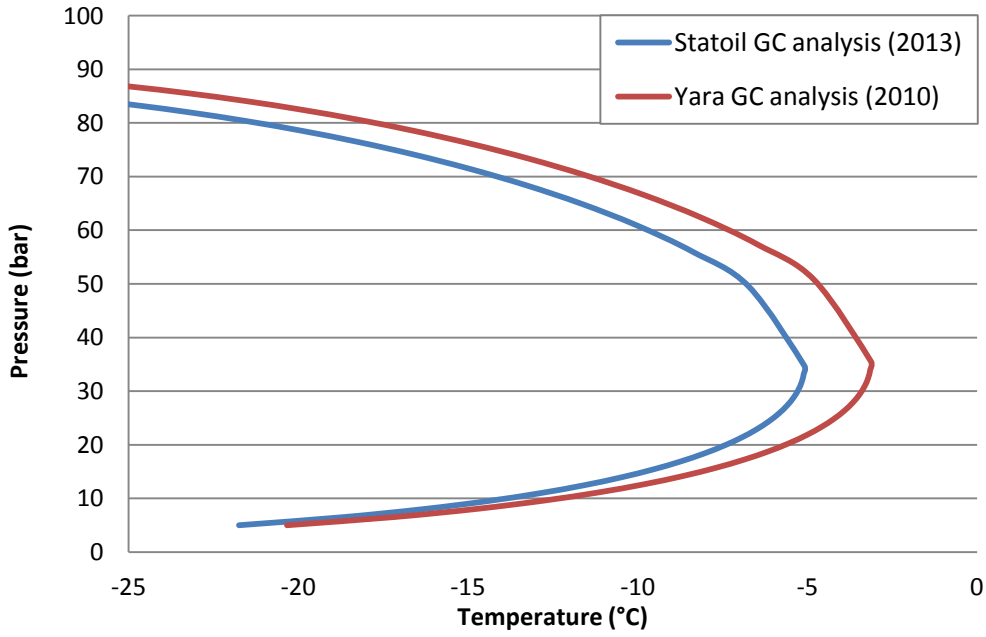

Figure 3.9: Effect of different composition for SNG 2 on phase envelope

Figure 3.9 illustrates the effect of the GC-analysis, shown in the table above, on the phase envelope. It is obvious that the difference in the compositions has a significant effect on the phase envelope. It is therefore decided that in the rest of the thesis the basis for the modelling work will be the compositions reported from the GC-analysis performed at Statoil.

– SNG 3

The difference in composition of SNG 3 and the effect of it on the phase envelope are shown in Table 3.7 and Figure 3.10 respectively.

Table 3.7: Composition of SNG 3

Yara GC analysis (2010)		*Statoil GC analysis (2013)*	
Component	**mol %**	**Component**	**mol %**
Carbon dioxide	0.287	Carbon dioxide	0.27901
Nitrogen	5.67	Nitrogen	5.77660
Methane	83.3	Methane	83.29466
Ethane	7.56	Ethane	7.58345
Propane	2.02	Propane	2.00043
i-Butane	0.31	i-Butane	0.25648
n-Butane	0.526	n-Butane	0.49794
i-Pentane	0.119	i-Pentane	0.10525
n-Pentane	0.144	n-Pentane	0.12592
n-Hexane	0.068	n-Hexane	0.05933
n-Heptane	0.0137	n-Heptane	0.01186
n-Octane	0.011	n-Octane	0.00905

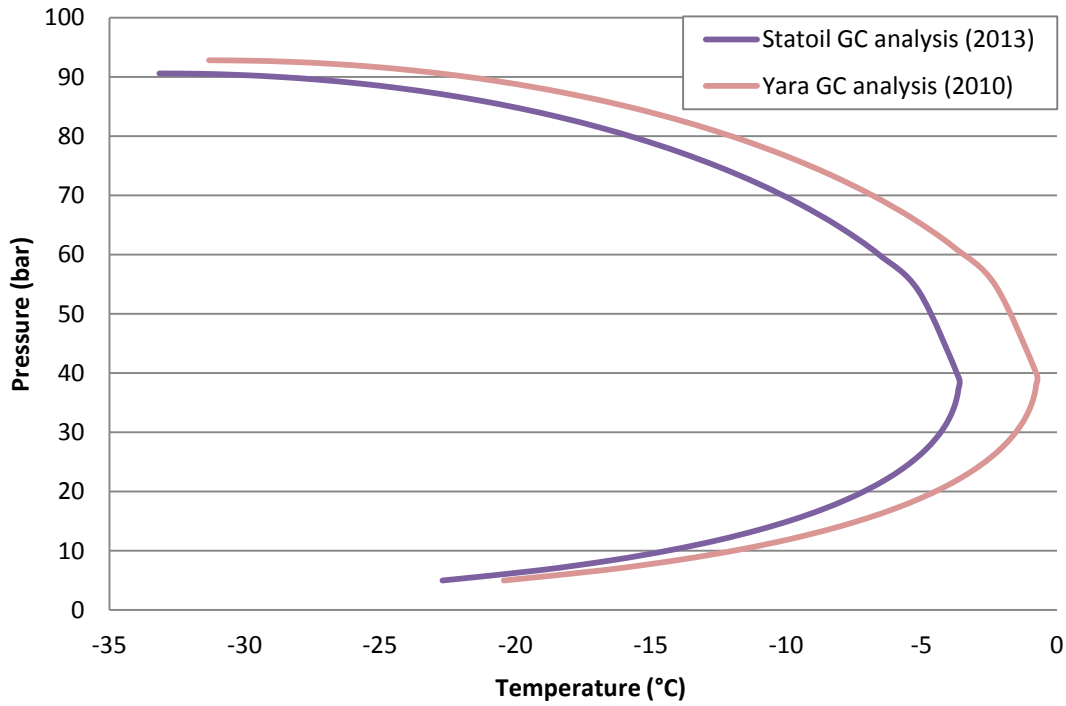

Figure 3.10: Effect of different composition for SNG 3 on phase envelope

It can be observed that the impact on the phase envelope of SNG 3 is also significant and, therefore, the composition reported from the GC-analysis will be used for SNG 3 as well.

It is observed that the mol % fraction of the heavy hydrocarbons has been decreased. The difference in composition presented for both synthetic gases could be explained based on adsorption theory. The heavier compounds might have been adsorbed onto the surface of the storage bottles making the gas richer.

– RG 1

The composition of RG1 was measured and is given in Table 3.8:

Table 3.8: Composition of RG1

Statoil GC analysis 2013	
Component	**mol %**
N2	0.55084
CO2	3.57606
C1	78.98930
C2	9.04769
C3	4.96121
iC4	0.68357
nC4	1.27920
2,2-dm-C3	0.01680
iC5	0.26699
nC5	0.28318
c-C5	0.01514
2,2-dm-C4	0.00307
2,3-dm-C4	0.00719
2-m-C5	0.05169
3-m-C5	0.02696
nC6	0.06810
Benzene	0.01764
c-C6	0.06446
nC7	0.04032
Toluene	0.01037
c-C7	0.02507
nC8	0.00794
m-Xylene	0.00232
c-C8	0.00195
nC9	0.00203
C10	0.00090

3.5. Repeatability

When studying the effect of various parameters on a measurement, the repeatability error needs to be determined. The repeatability error shows the variation of the measurement when the experiment is repeated under the same conditions. Therefore, the operator, the dew point apparatus and the sample gas are the same. Knowing the repeatability error is essential in order to draw safe conclusions concerning the effect observed.

SNG 3 and RG 1 were measured twice so as the uncertainty concerning the repeatability to be defined. The experimental data can be found in Appendix D. The experiments have been held using 600cc of gas and chamber's temperature of 45°C. No heating jacket was used to preheat the sample. The results are shown in Figures 3.11 to 3.12. The deviations were calculated where possible and are presented on Tables 3.9 and 3.10 for SNG 3 and RG 1 respectively.

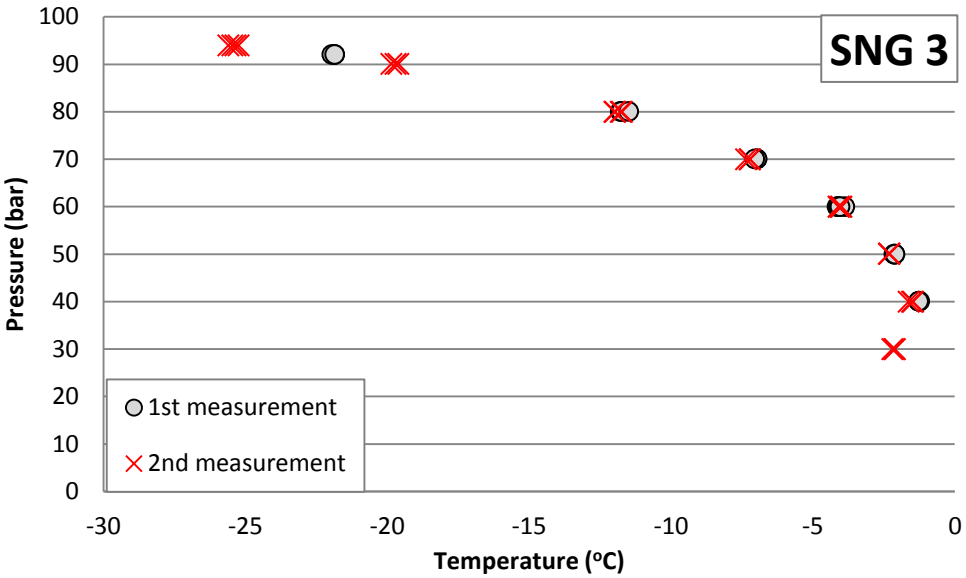

Figure 3.11: Repeatability test in SNG 3

Table 3.9: Deviations of the repeated dew points measured for SNG 3

	1st measurement	2nd measurement	Deviations
P (bar)	T (°C)	T (°C)	ΔT*
94	-	-25.4	-
92	-21.9	-	-
90	-	-19.7	-
80	-11.7	-11.9	0.2
70	-7.0	-7.3	0.3
60	-4.0	-4.1	0.1
50	-2.1	-2.3	0.2
40	-1.3	-1.6	0.3
30	-	-2.2	-

*ΔT= T_2nd measurement – T_1st measurement

Deviations can be calculated only in medium pressures, from 40 to 80 bar. At this pressure range, deviations vary from 0.1°C to 0.3°C. No particular tendency is noticed.

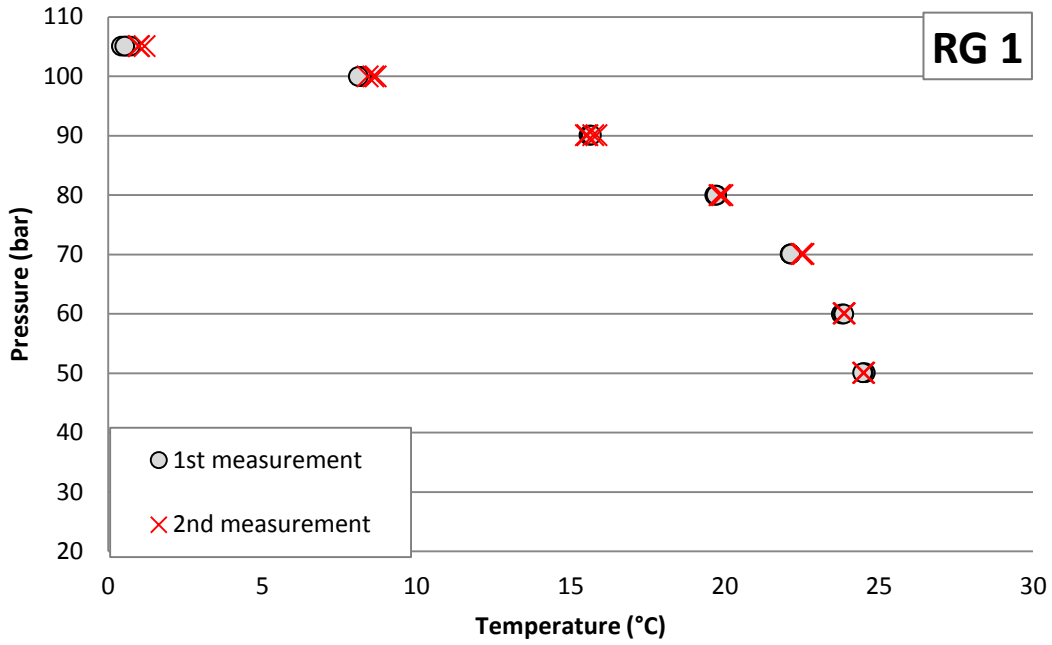

Figure 3.12: Repeatability test in RG 1

Table 3.10: Deviations of the repeated dew points measured for RG 1

	1st measurement	2nd measurement	Deviations
P (bar)	T (°C)	T (°C)	ΔT*
105	0.6	1.1	0.5
100	8.2	8.6	0.4
90	15.6	15.6	0.0
80	19.7	19.9	0.2
70	22.1	22.5	0.4
60	23.8	23.9	0.0
50	24.5	24.5	0.0

*ΔT= T_2nd measurement – T_1st measurement

Deviations are available at medium and high pressures. The deviations vary from 0.0°C to 0.5°C. No particular tendency is noticed.

Discussion

The deviations range, for SNG 3, from 0.1°C to 0.3°C and, for RG 1, from 0.0°C to 0.5°C. The calculation of deviations was possible only at medium pressures for SNG 3 and at medium and high pressures for RG 1. A particular tendency is not observed. However, my experience has shown that at high pressures near CCB the detection of the dew is very difficult and, therefore, high deviations were expected. The maximum deviation noticed during the repeatability test is considered a good indication of the experimental error for all gases. Thus, in the rest of this report, deviations observed up to 0.5°C will be considered within the experimental error.

3.6. Volume effect

The first parameter to be studied, as far as its effect on the accuracy of the dew point measurement is concerned, is the volume effect. All three gases were measured using 300cc and 600cc respectively. The choice of the volumes used to study this effect was based mainly on practical reasons; the available volume for real gases is 600cc to 800cc. The temperature of the chamber during the experiments was constant T=45^{o}C. No heating jacket was used to the samples. All experimental data are given in Appendix D.

It should be pointed out that the volume effect concerns the volume inserted inside GERG rig according to the volume of the pistons available. The volume of piping besides the pistons is considered negligible. Although the volume filled is constant at each experiment, the amount gas is different because the pressure of each gas bottle is different. Thus, given specific volume of gas, the moles inserted are fewer as the pressure is lower.

The volume effect is illustrated for all three gases in the figures below. Tables containing the deviations between the hydrocarbon dew points measured at each volume accompany the figures.

– SNG 2

The volume effect for SNG 2 is shown in Figure 3.13. The calculation of the deviations of the measured dew point temperatures follows (Table 3.11).

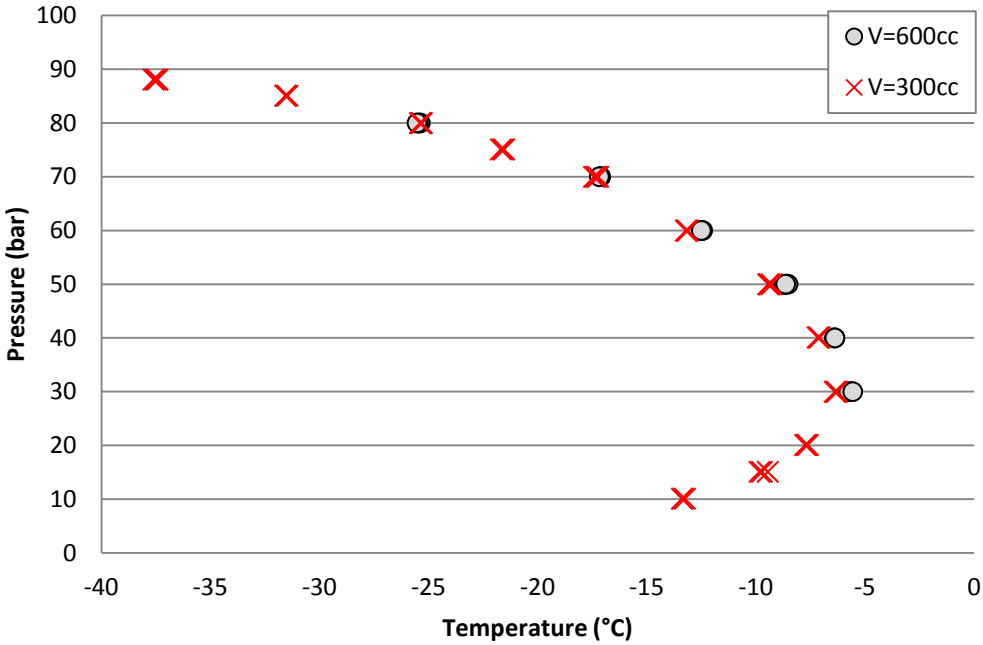

Figure 3.13: Volume effect in SNG 2

Table 3.11: Deviations of dew points measured in different volumes for SNG 2

	V1=600 cc	V2=300 cc	Deviations
P (bar)	T (^{o}C)	T (^{o}C)	ΔT*
88	-	-37.5	-
85	-	-31.5	-
80	-25.5	-25.3	-0.1
75	-	-21.6	-
70	-17.1	-17.3	0.2
60	-12.5	-13.2	0.7
50	-8.6	-9.4	0.7
40	-6.4	-7.1	0.7
30	-5.6	-6.3	0.7
20	-	-7.7	-
15	-	-9.7	-
10	-	-13.3	-

*ΔT= T_V1 – T_V2

Deviations can be estimated in medium pressures and up to 80 bar. The higher deviation and most often presented is 0.7°C with a minimum of 0.1°C. From 30 bar to 60 bar the deviation is the same ΔT=0.7°C.

– SNG 3

Figure 3.14 shows the volume effect for SNG 3. The deviations between the dew points measured in different volumes are presented in Table 3.12.

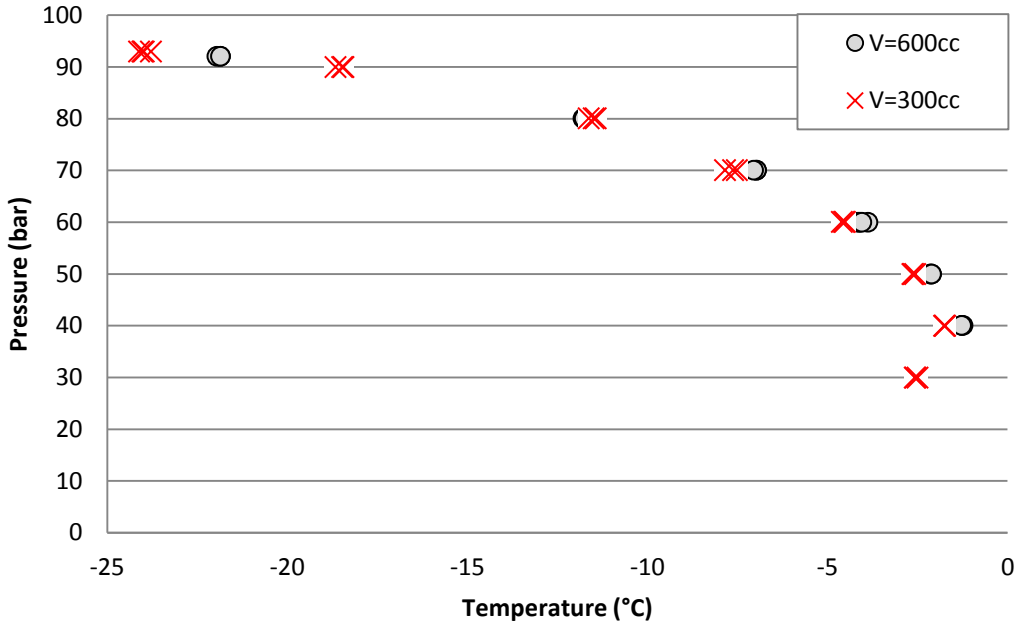

Figure 3.14: Volume effect in SNG 3

Table 3.12: Deviations of dew points measured in different volumes for SNG 3

	V1=600 cc	V2=300 cc	Deviations
P (bar)	T (^{o}C)	T (^{o}C)	ΔT*
93	-	-24.0	-
92	-21.9	-	-
90	-	-18.5	-
80	-11.7	-11.5	-0.2
70	-7.0	-7.7	0.7
60	-4.0	-4.6	0.5
50	-2.1	-2.6	0.5
40	-1.3	-1.8	0.5
30	-	-2.6	-

*ΔT= T_V1 – T_V2

Deviations are available at medium pressures. The range of the deviation is 0.2°C to 0.7°C. From 40 bar to 60 bar, the deviations are the same ΔT=0.5°C.

– RG 1

Figure 3.15 and Table 3.13 present, respectively, the volume effect and the deviations between the dew point temperatures of each experiment for RG 1.

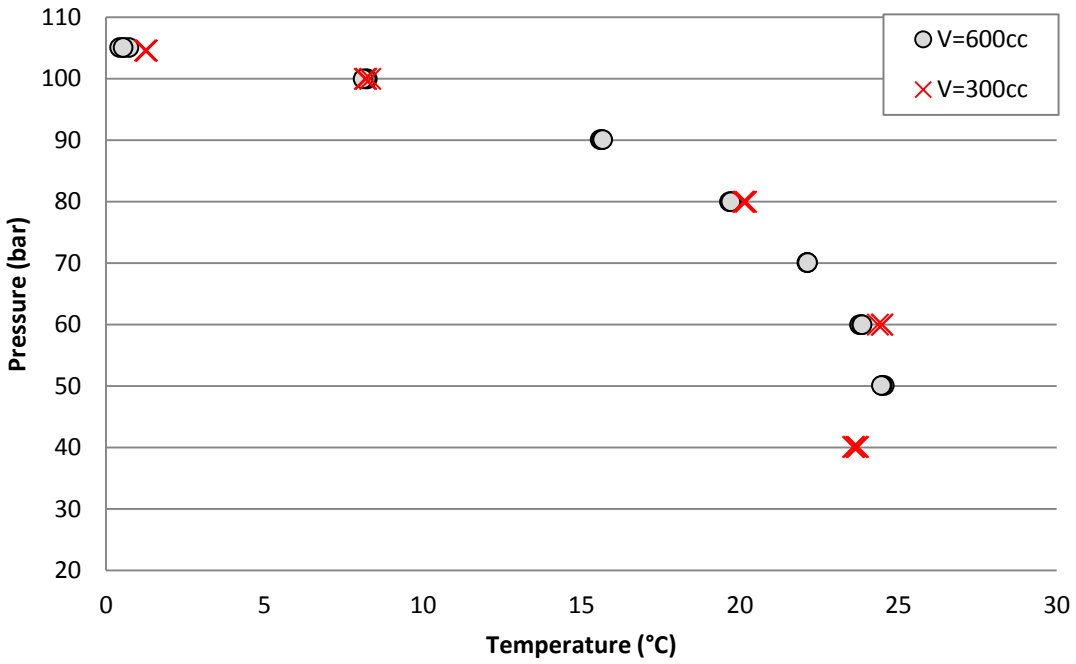

Figure 3.15: Volume effect in RG 1

Table 3.13: Deviations of dew points measured in different volumes for RG 1

	V1=600 cc	V2=300 cc	Deviations
P (bar)	T (^{o}C)	T (^{o}C)	ΔT*
105	0.6	1.3	-0.7
100	8.2	8.2	0.0
90	15.6	-	-
80	19.7	20.1	-0.4
70	22.1	-	-
60	23.8	24.4	-0.6
50	24.5	-	-
40	-	23.6	-

*ΔT= T_V1 – T_V2

The dew points measured with different volumes of gas being inserted inside the rig vary from 0 to 0.7°C. A tendency does not seem to exist.

– Discussion

To sum up, the deviations observed range from 0.0°C, 0.1°C and 0.2°C for RG 1, SNG 2 and SNG 3 respectively up to 0.7°C for all three gases. For SNG 2 and SNG 3 the measurements conducted using 600cc of gas seem to present a trend to have higher dew points than those measured with 300cc. This behavior would be in accordance with the adsorption theory as greater volume maximizes the ratio adsorption/surface and, therefore, minimizes adsorption. However, the experimental data obtained for RG 1 seem to show the opposite trend. In all cases, such behavior is not noticed near CCB.

The deviations concerning the volume effect are very close to the repeatability error (ΔT=0.5°C). As long as the accuracy of the thermometer used in the HCDP measurement is 0.2°C (see subsection 3.2), the deviation of approximately 0.7°C is considered within the experimental uncertainty. Therefore, volume effect between 600cc and 300cc does not seem to exist.

3.7. Temperature effect

The second parameter studied in order to estimate its effect on the accuracy of the dew point measurements is the temperature applied inside the chamber. According to the adsorption theory, the application of different temperatures inside the chamber is expected to present differentiations on the dew point measurements.

The temperature effect was studied at all three gases. The thermodynamic behavior of the gases was studied at two different temperatures; 35°C and 45°C. The experiments were conducted using constant volume of 600cc and without the use of heating jackets to the gas bottles. The experimental data can be found in Appendix D. Figures 3.16 to 3.18 and Tables 3.14 to 3.16 contain the results of this study.

– SNG 2

The temperature effect for SNG 2 as well as the deviations of the two series of measurements at 35°C and 45°C is presented below (Figure 3.16 and Table 3.14).

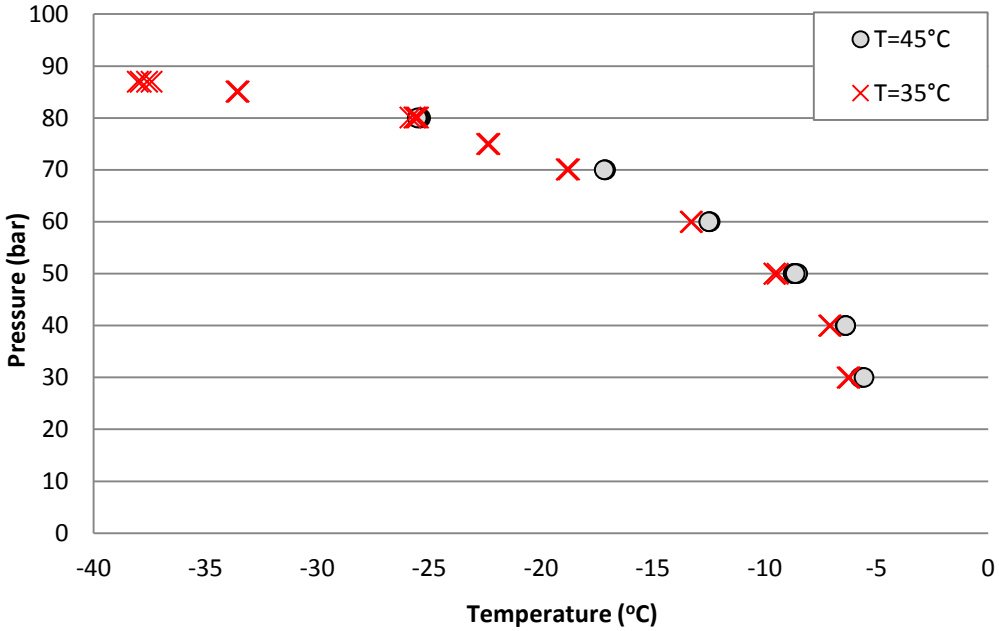

Figure 3.16: Temperature effect in SNG 2

Table 3.14: Deviations of the dew points measured in different chamber temperatures for SNG 2

	T1=45°C	T2=35°C	Deviations
P (bar)	T (°C)	T (°C)	ΔT*
87	-	-37.7	-
85	-	-33.6	-
80	-25.5	-25.7	0.2
75	-	-22.3	-
70	-17.1	-18.8	1.7
60	-12.5	-13.3	0.8
50	-8.6	-9.5	0.9
40	-6.4	-7.1	0.7
30	-5.6	-6.2	0.6

*ΔT= T_T1 – T_T2

Figure 3.16 shows the tendency of the dew points to move to the left when lower temperature is applied inside the chamber. This tendency is in accordance with the adsorption theory since the adsorption of heavy components leads to the movement of the dew point line to the left to lower temperatures. The effect is more obvious at medium pressures at which the deviations range from 0.6°C up to 1.7°C. As far as

higher pressures are concerned, only at 80 bar there are available data for both chamber temperatures, presenting a deviation of 0.2°C.

– SNG 3

Figure 3.17 and Table 3.15 present, respectively, the volume effect and the deviations between the dew point temperatures of each experiment for RG 1.

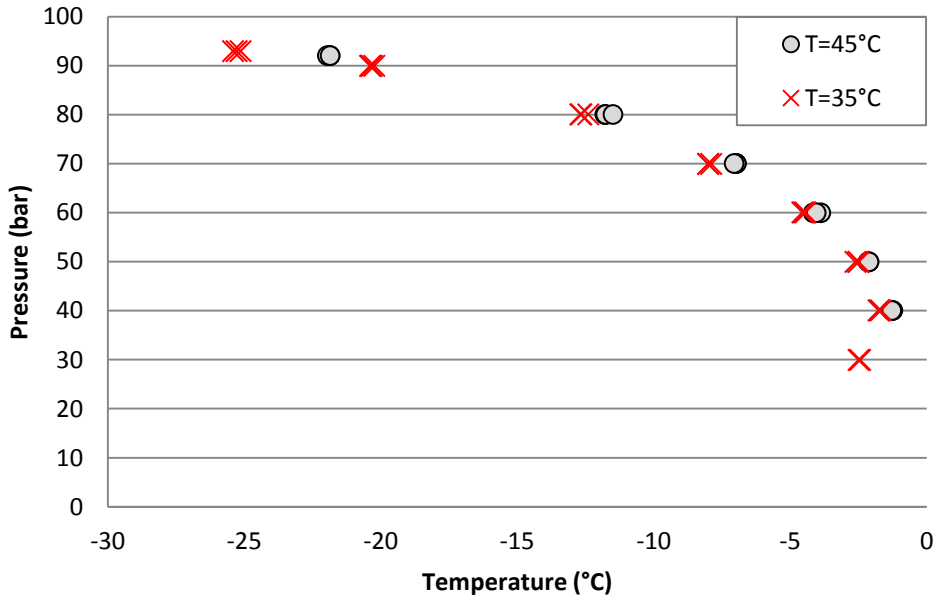

Figure 3.17: Temperature effect in SNG 3

Table 3.15: Deviations of the dew points measured in different chamber temperatures for SNG 3

	T1=45 °C	T2=35 °C	Deviations
P (bar)	T (°C)	T (°C)	ΔT*
93	-	-25.3	-
92	-21.9	-	-
90	-	-20.3	-
80	-11.7	-12.6	0.9
70	-7.0	-8.0	1.0
60	-4.0	-4.5	0.5
50	-2.1	-2.5	0.4
40	-1.3	-1.8	0.5
30	-	-2.5	-

*ΔT= T_T1 – T_T2

The tendency described earlier is clear on the SNG 3 measurements as well. Up to 80 bar the deviations range from 0.4°C to 1.0°C. At higher pressures, a comparison cannot be made because the pressure is not the same. Near CCB, the dew point curve is almost flat leading to great temperature differences even for very small pressure

changes. Since dew point measurements in the same pressure are not available, conclusions cannot be drawn about temperature effect near cricondenbar.

– RG 1

Figure 3.18 shows the volume effect for RG 1. The deviations between the dew points measured in different volumes are presented in Table 3.16.

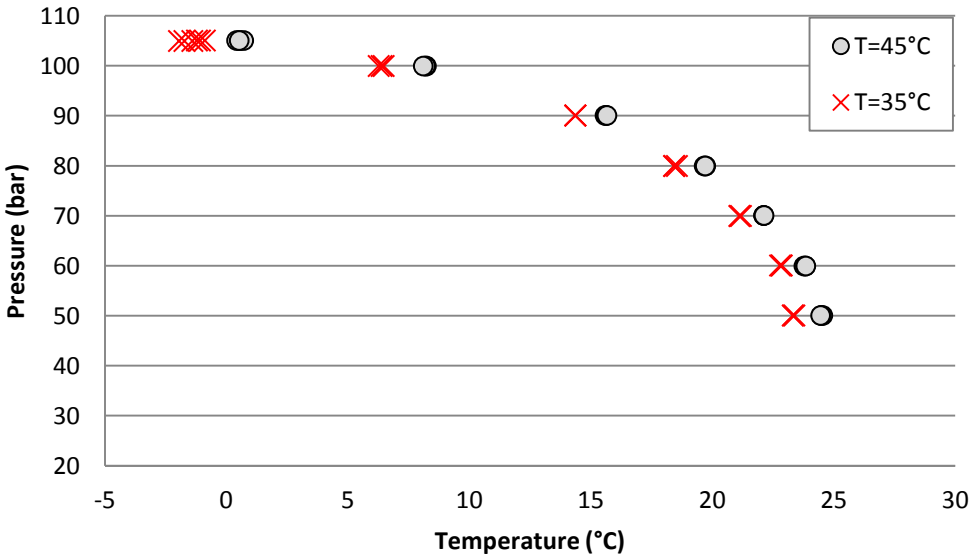

Figure 3.18: Temperature effect in RG 1

Table 3.16: Deviations of the dew points measured in different chamber temperatures for RG 1

	T1=45 °C	T2=35 °C	Deviations
P (bar)	T (°C)	T (°C)	ΔT*
105	0.6	-1.4	1.9
100	8.2	6.4	1.8
90	15.6	14.4	1.3
80	19.7	18.5	1.2
70	22.1	21.1	1.0
60	23.8	22.8	1.0
50	24.5	23.3	1.2

*ΔT= T_T1 – T_T2

As expected, since RG 1 contains heavier hydrocarbons than the synthetic gases employed in this work, the chamber's temperature effect is more pronounced. The deviations range from 1.0°C to 1.9°C and seem to increase as the pressure increases. This behavior is explained as near CCB the detection of the dew forming on the mirror is much more difficult than at lower pressures and, therefore, the observer's error is greater.

– Discussion

Based on the above, all three gases present the same tendency: the higher the temperature of the chamber is, the higher the hydrocarbon dew point temperature is measured. The deviations are higher for RG 1 with an average of 1.3°C whereas the average of the deviations for SNG 2 and SNG 3 are 0.8°C and 0.6°C respectively. It is clear that there is an effect of the chamber's temperature between 35 °C and 45 °C.

The tendency observed confirms the existence of adsorption phenomena inside the dew point apparatus. Adsorption occurs more readily in lower temperatures and decreases with increase in temperature. Thus, the higher the temperature of the chamber the less is the adsorption of the heavy hydrocarbons. The impact on the phase envelope is then smaller leading to more accurate measurements of the hydrocarbon dew points.

3.8. Sample Conditioning Effect

The sample conditioning effect was studied using the two out of three gases available in this work; SNG 2 and SNG 3. Mo more amount of RG 1 was available since it was all required for the study of volume and temperature effect. In this subsection, adsorption phenomena inside the storage bottles are studied. It is expected that, if adsorption is an issue inside the gas bottles, the measured dew points after the sample conditioning will be higher.

A heating jacket was used to heat the samples at 100°C for 12 hours before the filling of the rig. The temperature inside the chamber was 45°C and the volume filled was 600cc. The experimental data obtained from these experiments and the same conditions without heating of the samples, which are shown at Figures 3.19 and 3.20 for SNG 2 and SNG 3 respectively, can be found in Appendix D. Tables presenting the deviations of the two cases follow each figure.

– SNG 2

Figure 3.19 shows the volume effect for RG 1. The deviations between the dew points measured with different sample conditioning are presented in Table 3.17.

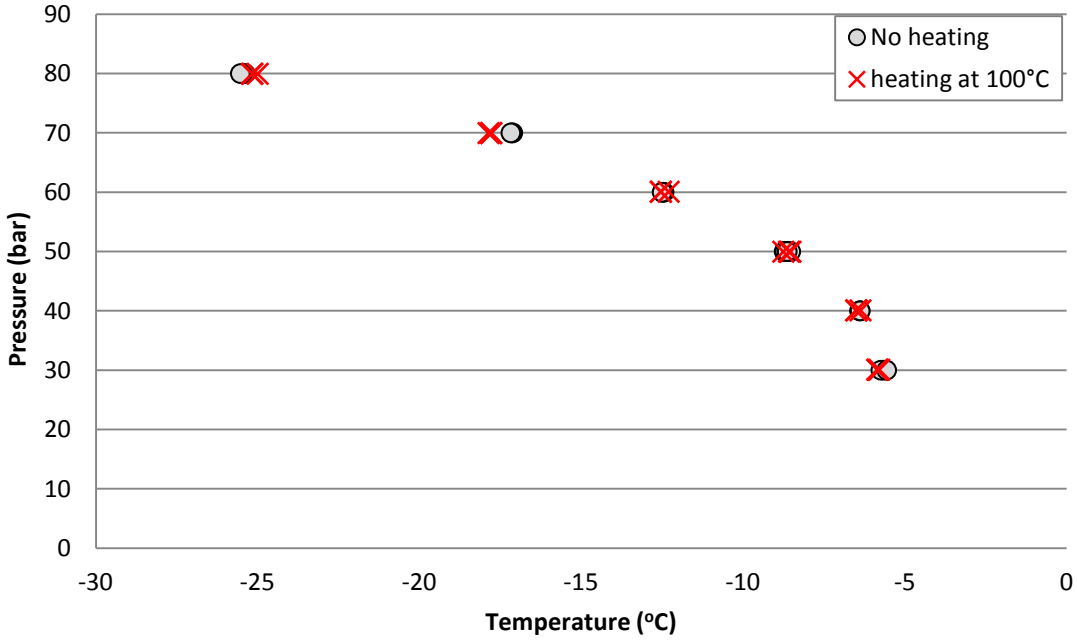

Figure 3.19: Sample conditioning effect in SNG 2

Table 3.17: Deviations of the dew points measured with and without preheating of the sample for SNG 2.

	No heating	Heating	Deviations
P (bar)	T1 (°C)	T2 (°C)	ΔT*
80	-25.5	-25.1	-0.3
70	-17.1	-17.8	0.7
60	-12.5	-12.5	0.0
50	-8.6	-8.6	0.0
40	-6.4	-6.5	0.1
30	-5.6	-5.8	0.2

*ΔT= T_Heating – T_No_heating

The sample conditioning effect on SNG 2 is not very clear. It seems that the dew points move slightly to the left at all pressures, except for 80 bar, when the sample has been preheated. The range of the deviations is 0°C to 0.7°C with an average deviation of 0.2°C.

– SNG 3

The temperature effect on SNG 3 is illustrated in Figure 3.20. Deviations on the dew point temperatures between the two series of experiments are presented in Table 3.19.

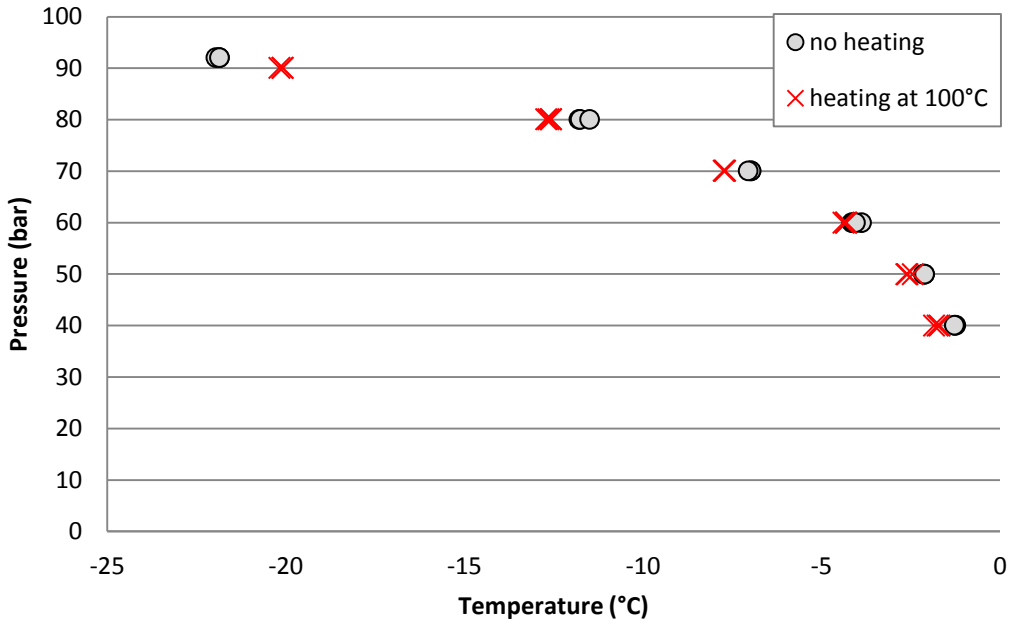

Figure 3.20: Sample conditioning effect in SNG 3

Table 3.18: Deviations of the dew points measured with and without preheating of the sample for SNG 3.

	No heating	Heating	Deviations
P (bar)	T1 (°C)	T2 (°C)	ΔT*
95	-	-27.9	-
92	-21.9	-	-
90	-	-20.1	-
80	-11.7	-12.6	0.9
70	-7.0	-7.7	0.7
60	-4.0	-4.3	0.3
50	-2.1	-2.6	0.4
40	-1.3	-1.8	0.5

*ΔT= T_Heating – T_No_heating

It seems like there is a tendency for the dew points to be lower when the sample gas has been preheated. However, a tendency is contrary to the expected behavior. In case the walls of the gas bottles adsorbed heavy components of the gas, the concentration of the heavy fraction inside the rig would be higher than the one during the measurements without sample conditioning. The deviation range for SNG 3 is from 0.3°C to 0.9°C

– Discussion

The sample conditioning effect is not clear. For both the gases measured, the dew point temperatures are measured slightly lower when the sample has been preheated at all pressures except for the dew point measured near CCB. The deviations for SNG 3 is range from 0.3°C to 0.9°C and are higher than those seen for SNG 2; yet, the average deviation is 0.6°C which is approximately equal to the repeatability error.

To summarize with, adsorption phenomena do not seem to be present in the gases' storage bottles. The average deviation for SNG 2 and SNG 3 is 0.2°C and 0.6°C respectively. Although, it seems that the different dew points measured are within the experimental uncertainty, the unexpected tendency of SNG 3 require further study as a means to draw safer conclusions.

4. Modelling

The composition deriving from the gas chromatograph analysis is used as an input for the three thermodynamic models employed in this work: SRK, PC-SAFT and UMR-PRU. The reliability of the models is evaluated according to the experimental dew points measured in this work. In addition, the effect of the uncertainty of the composition deriving from the GC analysis is studied through a Monte Carlo simulation.

4.1. Modelling of gases

SRK, PC-SAFT and the more advanced thermodynamic model, UMR-PRU, are evaluated based on the dew point measurements. Aiming to evaluate how well the model describes measured dew points, the interaction parameter k_{ij} is considered equal to 0. The experimental data chosen to evaluate the reliability of the models are those that seem to be the least affected by adsorption phenomena. These are the hydrocarbon dew point measurements conducted at chamber's temperature of 45°C and using 600cc of the sample gas without sample conditioning. All experimental data can be found in Appendix E.

4.1.1. Modelling of SNG 2

SNG 2 is a binary mixture consisting primarily of the light component of methane and the some traces of n-heptane (see Table 3.5). The predictions of the dew point curve as well as the experimental data are presented in Figure 4.1.

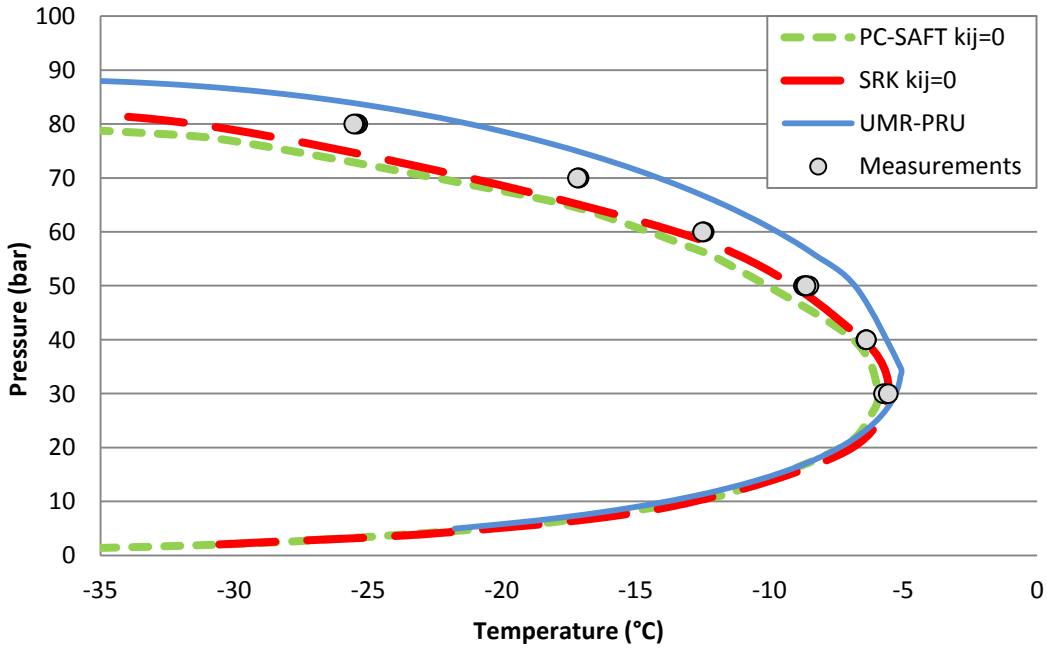

Figure 4.1: Predicted dew point curves for SNG 2 with the SRK, PC-SAFT and UMR-PRU models

SRK and PC-SAFT models predict similar dew points except from the higher pressures at which SRK predicts higher dew points than PC-SAFT. The three models predict almost identically the dew point curve up to 20 bar. UMR-PRU predicts higher dew points above 30 bar. The deviation between the UMR-PRU predictions and SRK, PC-SAFT predicted dew points increase as the pressure increases.

No conclusions can be drawn concerning the reliability of the models at low pressures since experimental data are not available. At medium pressures, SRK and PC-SAFT approach well the measured dew points with SRK being slightly better than PC-SAFT. UMR-PRU overestimates all experimental data. However, UMR-PRU seems to provide better cricondenbar (CCB) prediction than SRK and, of course, PC-SAFT.

4.1.2. Modelling of SNG 3

SNG 3 is a multi-component mixture similar to a real gas composed by both non-hydrocarbons and heavy hydrocarbons up to n-octane. Figure 4.2 illustrates the predicted and measured hydrocarbon dew points.

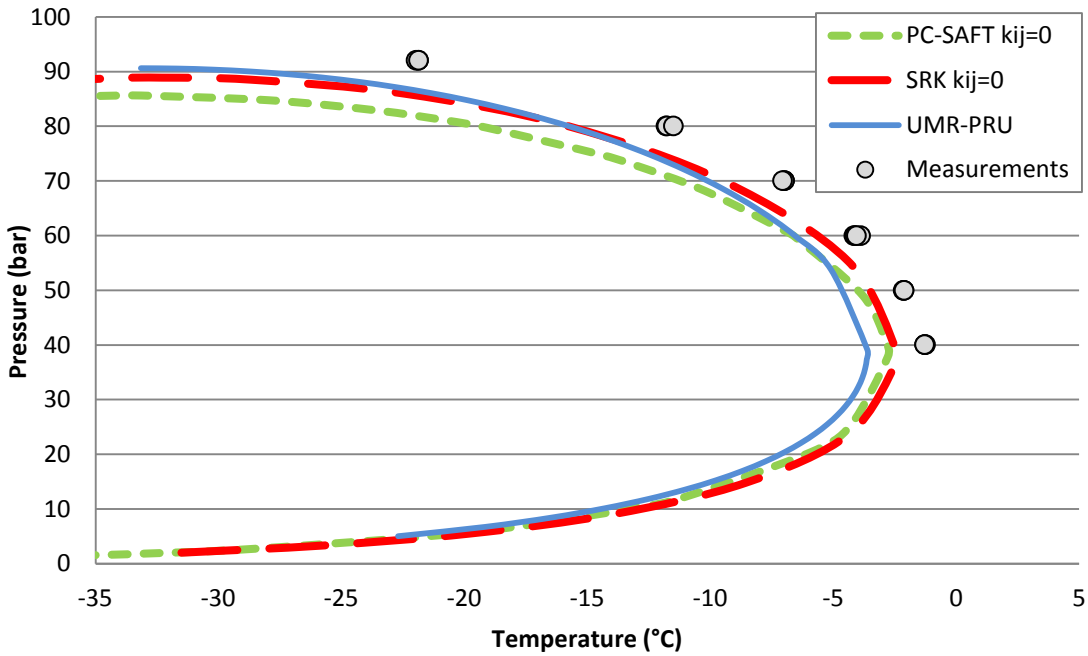

Figure 4.2: Predicted dew point curves for SNG 3 with the SRK, PC-SAFT and UMR-PRU models

All three models underestimate the measured dew points for SNG 3. At low pressures, below 20 bar all three models predict very similar dew points. At medium pressures and near the CCT, SRK and PC-SAFT predict similarly the dew point curve whereas UMR-PRU underestimates those predictions. SRK and PC-SAFT approach better the experimental dew points than UMR-PRU which underestimates them significantly. At

high pressures, UMR-PRU is similar to SRK, and yields again the best CCB prediction while PC-SAFT underpredicts again the dew point temperatures.

4.1.3. Modelling of RG 1

The third gas studied is a real gas consisting of nitrogen, carbon dioxide and hydrocarbons from methane to n-decane. The predictions of the dew point curve as well as the experimental data are presented in Figure 4.3.

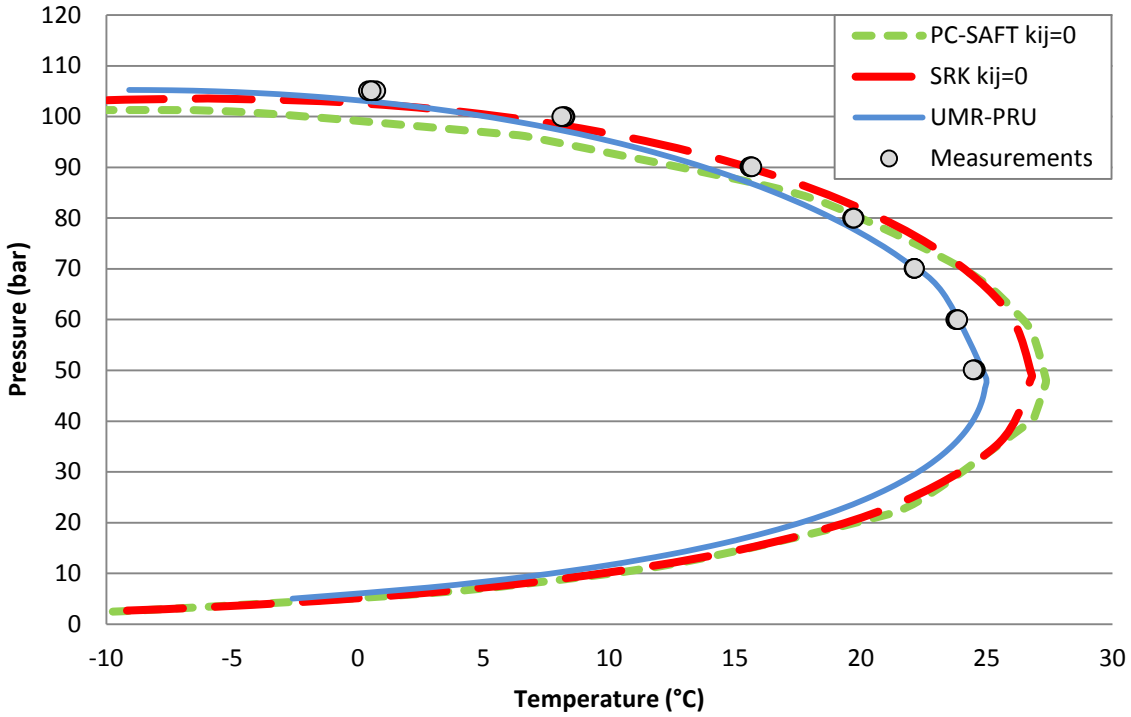

Figure 4.3: Predicted dew point curves for RG 1 with the SRK, PC-SAFT and UMR-PRU models

At low pressures, below 20 bar, the three models are similar again. At medium pressures and closer to CCT, SRK and PC-SAFT predict similar dew points overpredicting the experimental data while the UMR-PRU CCT prediction is approaches very well the measured dew point temperature. At high pressures and near the CCB the models approach better the dew points in the order UMR-PRU > SRK > PC-SAFT.

4.2. Uncertainty analysis

4.2.1. Uncertainty in GC-analysis

A Monte Carlo simulation is carried out to evaluate the effect of the uncertainties in the gas analysis on the simulated phase envelope. UMR-PRU was chosen for the performance of this uncertainty analysis.

Monte Carlo simulation picks random normally distributed values in order to generate a new composition. This sampling allows an uncertainty band to be defined. Ten repeated samples were taken at each pressure level. Requirement for such uncertainty analysis is the input of the total analytical uncertainty of each component at GC determination ($U_{X(ANA)}$). $U_{X(ANA)}$ is a function of the uncertainty in GC-areas of repeated injections of the unknown sample (U_X), the uncertainty in GC-areas of repeated injection of the reference gas (U_R) and the certified uncertainty of each component in the used reference gas (U_C). U_X and U_R values were found in literature and are always equal [1]. The uncertainties are given in Table 4.1.

Table 4.1: Uncertainty in GC-areas of repeated injections

Concentration range (mole)		Max. allowed deviation
MIN	MAX	relative %
1 ppm	5 ppm	20
5 ppm	10 ppm	10
10 ppm	0.01%	5
0.01%	0.10%	4
0.10%	1%	3
1%	10%	2
10%	50 %	1
50%	100 %	0.5

The simulations results together with the experimental dew points are given in Figures 4.4 to 4.6.

– SNG 2

The effect of the uncertainties in the GC analysis for SNG 2 is illustrated in Figure 4.4.

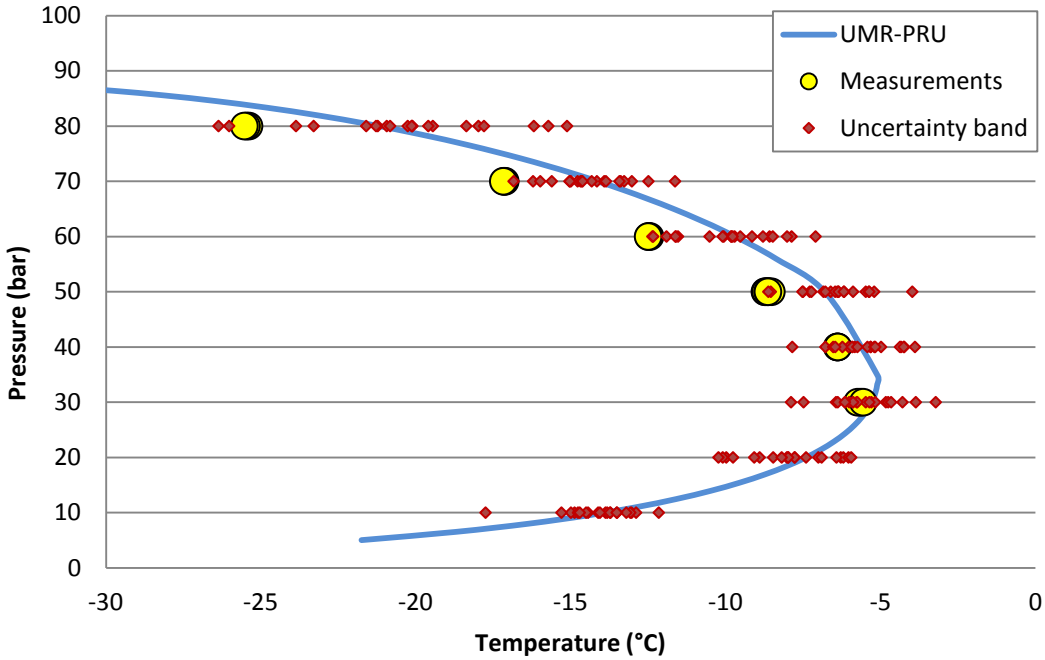

Figure 4.4: Effect of uncertainties in the gas analysis of the simulated phase envelope for SNG 2

All experimental data are within the uncertainty in the chromatographic analysis except for the measured dew point at 70 bar. A trend is indicated according to which as pressure increases, the measurements are moving to the inner band of uncertainty while around CCT they are almost in the middle of the range. The maximum deviation indicated in the simulated dew points is 6.1°C. The range is wide due to the very low concentration of n-heptane. The lower the concentration of the component is, the higher the relative % deviation (Table 4.1).

– SNG 3

The results from Monte Carlo simulation on SNG 3, as far as the effect of the uncertainty in composition is concerned, are shown in Figure 4.5.

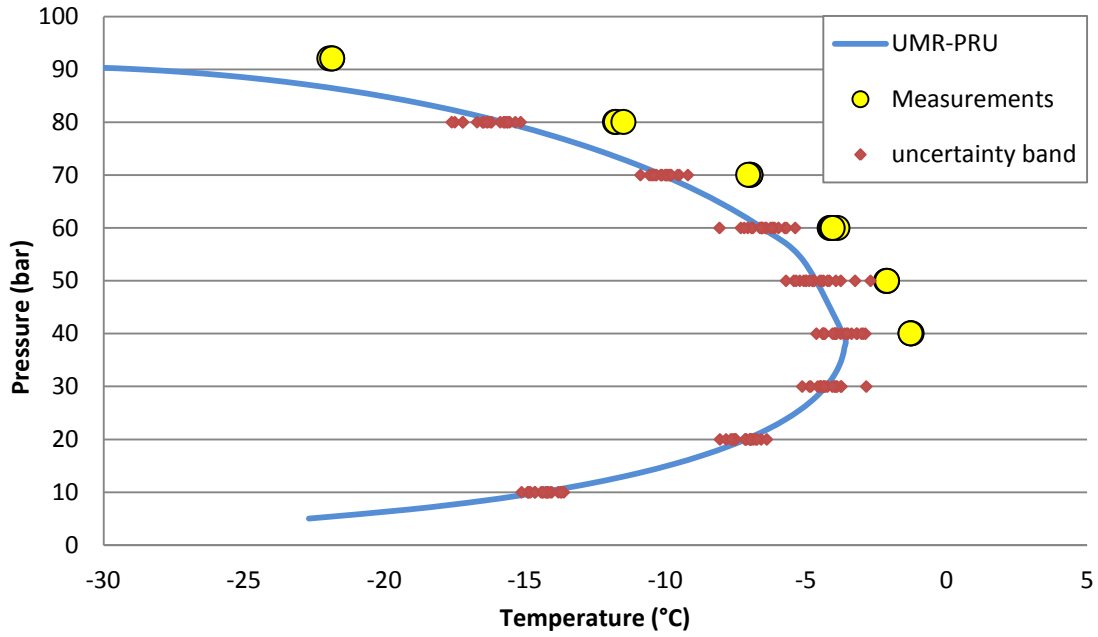

Figure 4.5: Effect of uncertainties in the gas analysis of the simulated phase envelope for SNG 3

The simulation show that the uncertainty in the chromatographic analysis for SNG 3 is not enough to explain the difference between the experimental and simulated phase envelope as the calculated dew points do not cover the experimental dew points. Experimental data are outside the range at all pressures. In general, the maximum deviation (2.6°C) appears at the highest pressure again.

– RG 1

Figure 4.6 shows the effect of the uncertainties in the GC analysis for RG 1.

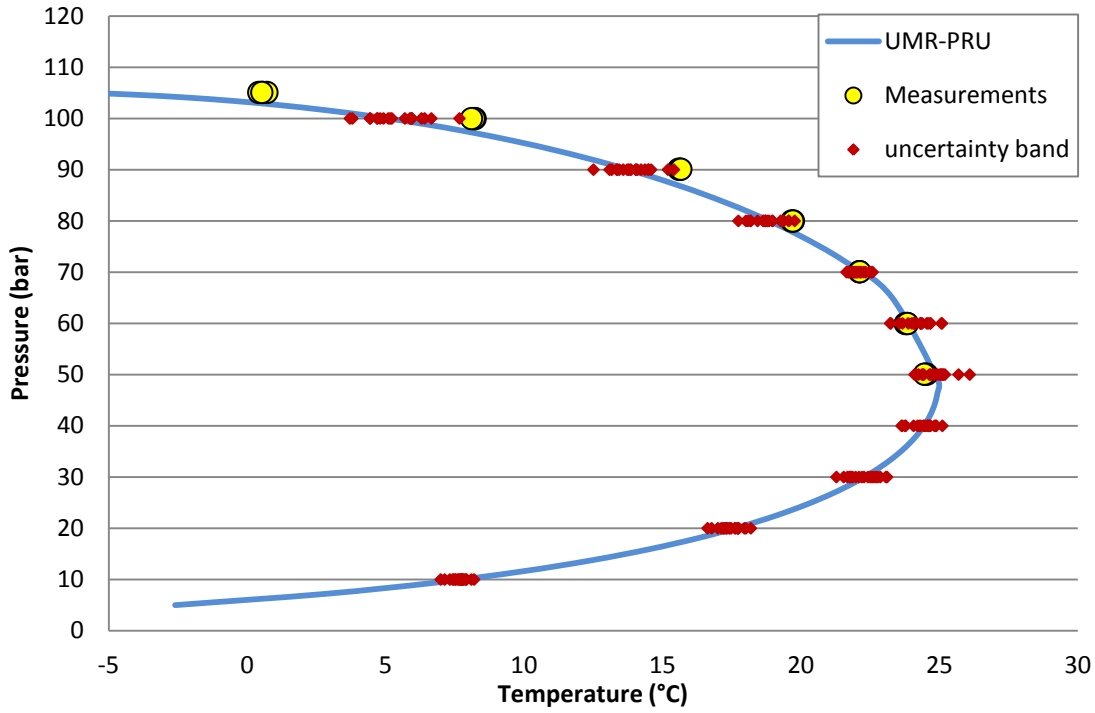

Figure 4.6: Effect of uncertainties in the gas analysis of the simulated phase envelope for RG 1

It is indicated that the measured dew points are clearly within the uncertainty in composition at medium pressure whereas they move to move to the outer band of uncertainty as pressure increases. The maximum deviation of 2.7°C is noticed at the highest pressure calculated.

It is worth mentioning that for the real gas a certified uncertainty of each component is obviously not available. The value for U_C was assumed equal to U_X and U_R (Table 4.1). These values are lower than those of the certified value of a synthetic gas such as SNG 2 and SNG 3 (Appendix F). Thus, the smaller band of uncertainty noticed for RG 1 compared with SNG 2 and SNG 3 is expected.

– Discussion

Based on the above calculations, the measurement of SNG 2 is the only, out of the measurement of the three gases employed in this work, which is within the uncertainty of the simulated phase envelope. Experimental dew points for SNG 3 cannot be predicted accurately even if the GC uncertainty is taken under consideration whereas UMR-PRU predictions for RG 1 are within the composition uncertainty only in medium pressures. At all three cases, a smaller uncertainty band is observed at low pressures which gets wider as the pressure increases and the system becomes more unstable.

4.2.2. Uncertainty in the experimental measurement

The dew point measurements contain the uncertainty deriving from the chromatographic gas analysis as well as the experimental error in the dew point measurement itself. This error has already been approached as the repeatability error of 0.5°C (see subsection 3.4). Nevertheless, there are more uncertainties to take under consideration during the evaluation of the reliability of a thermodynamic model. First, the uncertainties deriving from the pressure and temperature indicators which are both approximately 0.2°C. Secondly, and most significantly, the uncertainty as far as the dew detection is concerned. The observer's error is high, especially at high pressures near CCB, and cannot be precisely determined.

The presence of all the above mentioned uncertainties leads to the conclusion that, although the experimental uncertainty cannot be quantified, it is probably higher than 0.5°C.

Figures 4.7 to 4.9 show the experimental uncertainty together with the uncertainty band deriving from the gas analysis.

– SNG 2

Both the uncertainty from the gas analysis with GC and the experimental error of the dew point measurement are shown in Figure 4.7

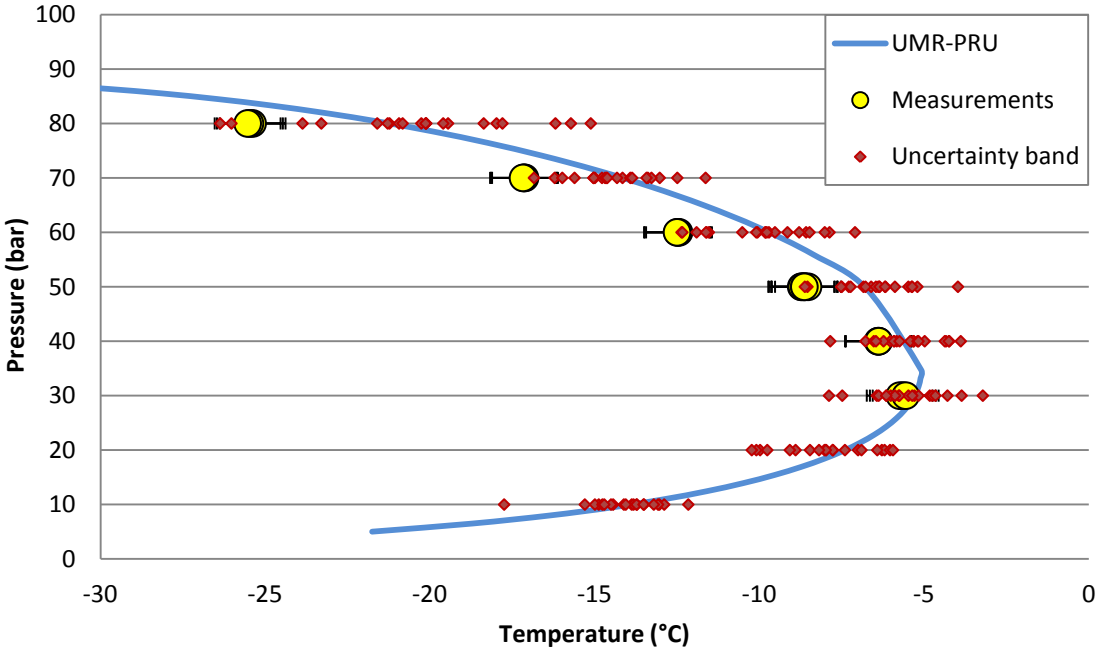

Figure 4.7: Effect of experimental (black spots) and chromatographic gas analysis uncertainties (red spots) for SNG 2

It is indicated that the experimental data for SNG 2 are clearly within the uncertainty from the GC analysis together with the experimental error in the experimental point itself.

– SNG 3

Figure 4.8 shows also the effect of the GC analysis and the experimental uncertainty on the predicted phase envelope.

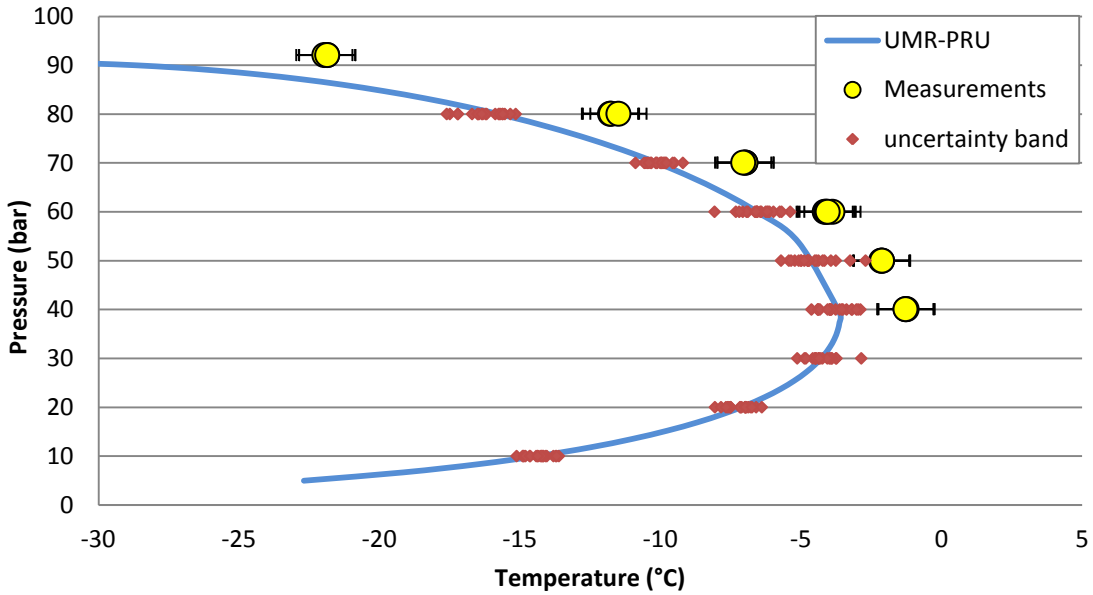

Figure 4.8: Effect of experimental (black spots) and chromatographic gas analysis uncertainties (red spots) for SNG 3

Figure 4.8 shows that the measured dew points for SNG 3 cannot be accurately predicted even when the experimental uncertainty is considered. At high pressures, the deviations remain significant and the measured dew points are not approached adequately.

– RG 1

The results of the uncertainty analysis on a dew point measurement are illustrated in Figure 4.9.

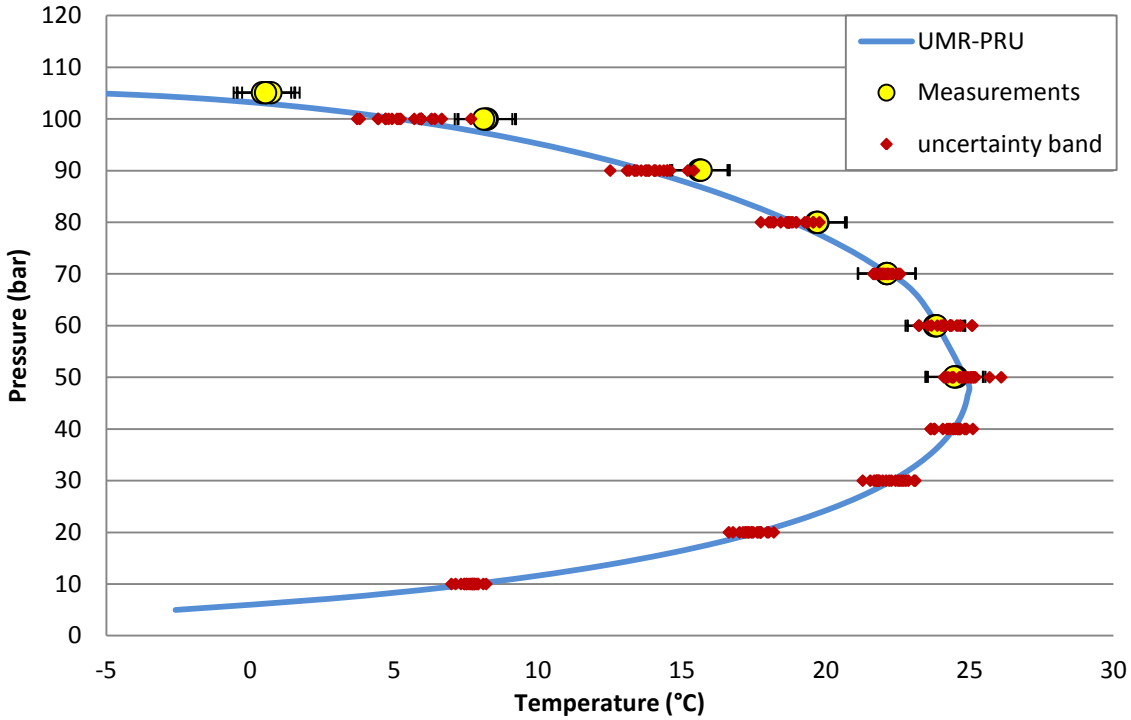

Figure 4.9: Effect of experimental (black spots) and chromatographic gas analysis uncertainties (red spots) for RG 1

This figure is further confirming the reliability of the model by presenting an accurate approach of the measured dew point temperatures within, not only the GC analysis' uncertainty, but also the experimental error.

– Discussion

Taking into account the experimental uncertainty as well as the effect of the uncertainty derived from the GC analysis of each gas, UMR-PRU model's reliability is further confirmed. SNG 2 and RG 1's dew point lines are adequately predicted while SNG 3 experimental data were better approached. Considering the always present undefined observer's error , it can safely be assumed UMR-PRU is a reliable model for dew point predictions for all three gases.

5. Conclusions

Based on the experimental data obtained in the frame of this diploma thesis and the presented discussions, various conclusions can be drawn concerning the parameters affecting the accuracy of the dew point measurements as well as the reliability of the thermodynamic models employed in this work.

- Even though the GERG rig has been made from materials designed in order to avoid/minimize adsorption phenomena, such phenomena seem to exist as indicated from the dew point measurements testing the chamber's temperature effect. The temperature effect is clear and in agreement with adsorption theory. As it was expected, at lower chamber temperature, where adsorption phenomena are more intense, dew point temperatures are recorded to be lower. This means that between 35 °C and 45 °C, measurements are more accurate at a chamber's temperature of 45 °C.
- Volume effect does not exist between measurements with 300cc and 600cc. The deviations noticed are within the experimental uncertainty. Higher volume of gas means higher volume to surface ratio. Thus, taking into consideration the presence of adsorption phenomena inside the dew point apparatus, employment of 600cc of sample gas is suggested for accurate dew point measurements.
- Sample conditioning does not seem to have an effect on the accuracy of the dew point measurements. The effect observed lies within the experimental uncertainty which points out that adsorption is not an issue inside storage bottles. However, the unexpected behavior of SNG 3 requires further study as a means to draw safer conclusions.

Based on the above, it is suggested that hydrocarbon dew point measurements in the GERG rig should be held when the chamber's temperature is 45°C and 600cc of sample gas are used. Preheating of the sample bottle is not required.

All three models employed in this work, SRK, PC-SAFT and UMR-PRU, seem to yield good hydrocarbon dew points and, therefore, are considered reliable.

The UMR-PRU is more accurate than SRK and PC-SAFT EoS at high pressures and seems to predict quite well the cricondenbar. On the other hand, SRK and PC-SAFT Eos are more accurate than UMR-PRU at pressures near cricondentherm in the case of SNGs. In the case of the real gas though, the UMR-PRU is the best in predicting the dew points and both CCB and CCT.

The SRK and PC-SAFT EoS predict similarly the phase envelope for all gases tested near CCT and at medium pressures and, sometimes, higher. At high pressures, both models underpredict the dew point temperatures and consequently the CCB, where

PC-SAFT is slightly worse than SRK. SRK and PC-SAFT are better than UMR-PRU in cricondentherm, which can still be considered reliable. UMR-PRU is the most reliable model of the three at high pressures, near cricondenbar.

The reliability of UMR-PRU is further supported through the uncertainty analysis performed. The total experimental uncertainty of the dew point measurement cannot be quantified as it contains, besides the repeatability error, the error of pressure indicators and the error from temperature indicators, the undefined observer's error. Monte Carlo simulation for the determination of the uncertainty range from the GC analysis indicates greater uncertainties as pressure increases. Experimental data which are not predicted with high accuracy are within the experimental uncertainty for all three gases.

6. Future Work

The temperature of the chamber was proven to have an impact on the dew point measurements. The performance of further experiments, conducted in higher pressures such as 60°C, could lead to a minimum effect of the adsorption and therefore more accurate dew points could be measured.

The sample conditioning effect was not very clear. The results showed the opposite behavior than the expected. Further experimental work is suggested in order to determine whether there is a consistency in such behavior that needs to be studied further.

In addition, more final conclusions regarding the effect of the different parameters studied in this diploma thesis could be made if a GC analysis of each studied gas could be available after the completion of the experiment.

Experimental data for SNG 3 were outside the dew point curves predicted by all three models at all pressures. An additional GC analysis of SNG 3 should be conducted to eliminate the possibility that the composition used was not representative of the gas. In case the composition is measured similarly, measurements of synthetic gases with similar compositions should be performed to see whether the measured dew points will present the same tendency. Then safer conclusions could be drawn regarding the reliability of the models for such natural gases.

Moreover, it was noticed that the temperature of the two pistons was different. A solution to this could be the installation of a fan inside the rig to ensure temperature homogeneity at the chamber.

Finally, a heat trace should be used on the CO_2 piping to avoid ice formation in the interior. The dry ice formed is clogging the piping and the cooling of the mirror stops until the temperature rises significantly. As a result, the conduction of the experiment is difficult and time-consuming. A heat traced piping could be the solution to this problem.

References

[1] http://www.naturalgas.org/, (2013)
[2] B. H. Rusten, L. H. Gjertsen, E. Solbraa, T. Kirkerød, T. Haugum and S. Puntervold, "Determination of the phase envelope – Crucial for process design and problem solving", GPA Annual Conference, (2008), Grapevine, Texas, USA.
[3] Anders Møllegaard Knage-Rasmussen, "Measurement and modelling of hydrocarbon dew points for synthetic and real natural gases", Master Thesis DTU, (2010).
[4] G. Soave, Chem. Eng. Sci., 27 (1972) 1197.
[5] J. Gross, G. Sadowski, Ind. Eng. Chem. Res. 40 (2001) 1244-1260.
[6] V. Louli, G. Pappa, Ch. Boukouvalas, S. Skouras, E. Solbraa, K.O. Christensen, E. Voutsas, Fluid Phase Equil., 334 (2012) 1.
[7] D. P. Tassios, "Applied chemical engineering thermodynamics", (1993).
[8] J. Herring, "Hydrocarbon Dew Point Is A Critical Consideration For Pipeline Operations", Pipeline & Gas Journal, 237 (2010)
[9] Nefeli Novak, "Development of characterization methods for the heavy (C6+) fraction of natural gases", Master Thesis, NTUA, (2013)
[10] http://folk.ntnu.no/helgemol/e-notes/PVT-Papers/SPEPBM-Ch5.pdf
[11] D.Y. Peng, D.B. Robinson, Ind. Eng. Chem. Fund., 15 (1976) 59.
[12] A. Brown, et. al, "Comparison of Methods for the Measurement of Hydrocarbon Dew Point of natural gas", UK: National Physical Laboratory, (2007) 49.
[13] API "Manual of Petroleum Measurement Standards", Chapter 14.1.
[14] http://chemwiki.ucdavis.edu/Analytical_Chemistry/Instrumental_Analysis/Chromatography/Gas_Chromatography
[15] J. D. Van der Waals, "Over de constinuiteit van den gas-en vloeistoftoestand", Doctoral Dissertation, (1873) Leiden, Holland.
[16] M. S. Graboski, T. E. Daubert, "A Modified Soave Equation of State for Phase Equilibrium Calculations. 1 Hydrocarbon Systems", Ind. Eng. Chem. Process Des. Dev., 17 (1978) 443.
[17] W. G. Chapman, G. Jackson, K. E. Gubbins, "Phase Equilibria of Associating Fluids. Chain Molecules with Multiple Bonding Sites", Mol. Phys., 65 (1988) 1057.
[18] W. G. Chapman, K. E. Gubbins, G. Jackson, M. Radosz, "New Reference Equation of State for Associating Liquids", Ind. Eng. Chem. Res., 29 (1990) 1709.
[19] H. K. Hansen, B. Goto, B. Kuhlmann, Institut for Kemiteknik, DTH, Lyngby, Denmark, SEP 9212, 1992
[20] E. Voutsas, K. Magoulas, D. Tassios, Ind. Eng. Chem. Res. 43 (2004) 6238
[21] http://webbook.nist.gov/chemistry/

Appendices

Appendix A: Experimental Procedure in detail
Appendix B: Pressure and temperature calibration
Appendix C: Ethane data
Appendix D: Experimental data
Appendix E: Predicted dew points from modelling
Appendix F: Certified uncertainties of GC analysis

Appendix A: Experimental Procedure in detail

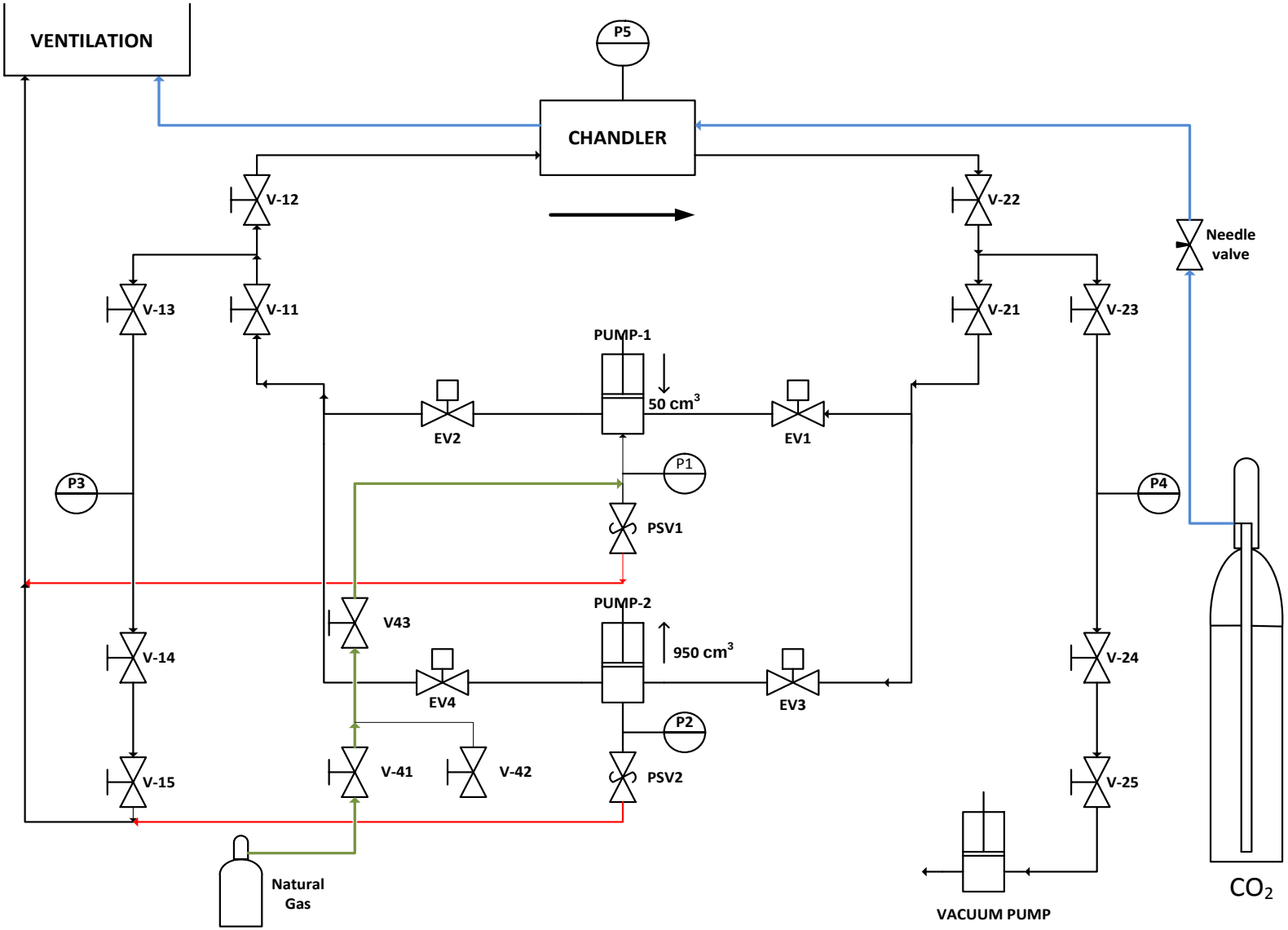

Figure 8.1: Process Flow Diagram of experimental apparatus

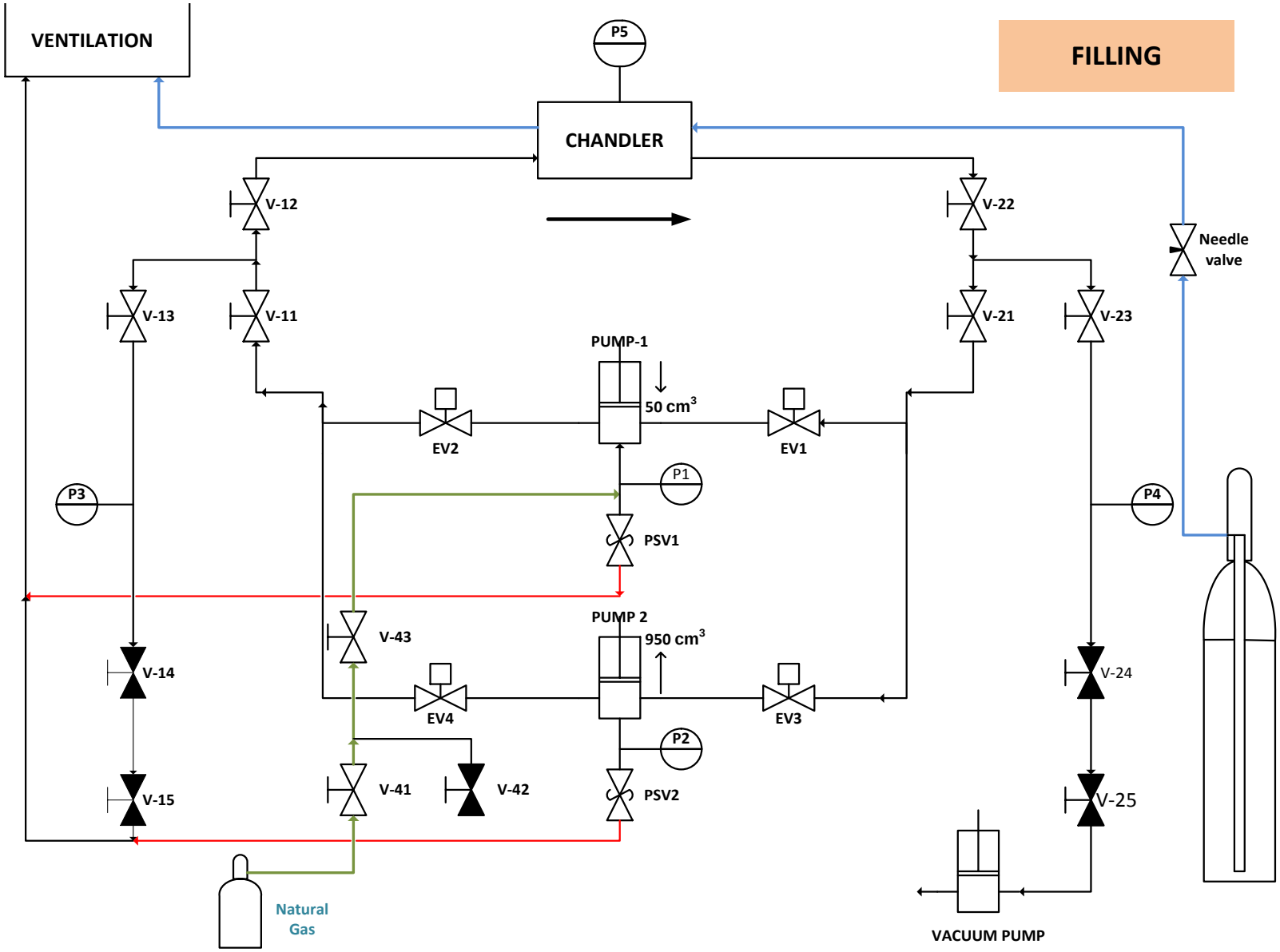

Figure 8.1: Process Flow Diagram of experimental apparatus during filling procedure

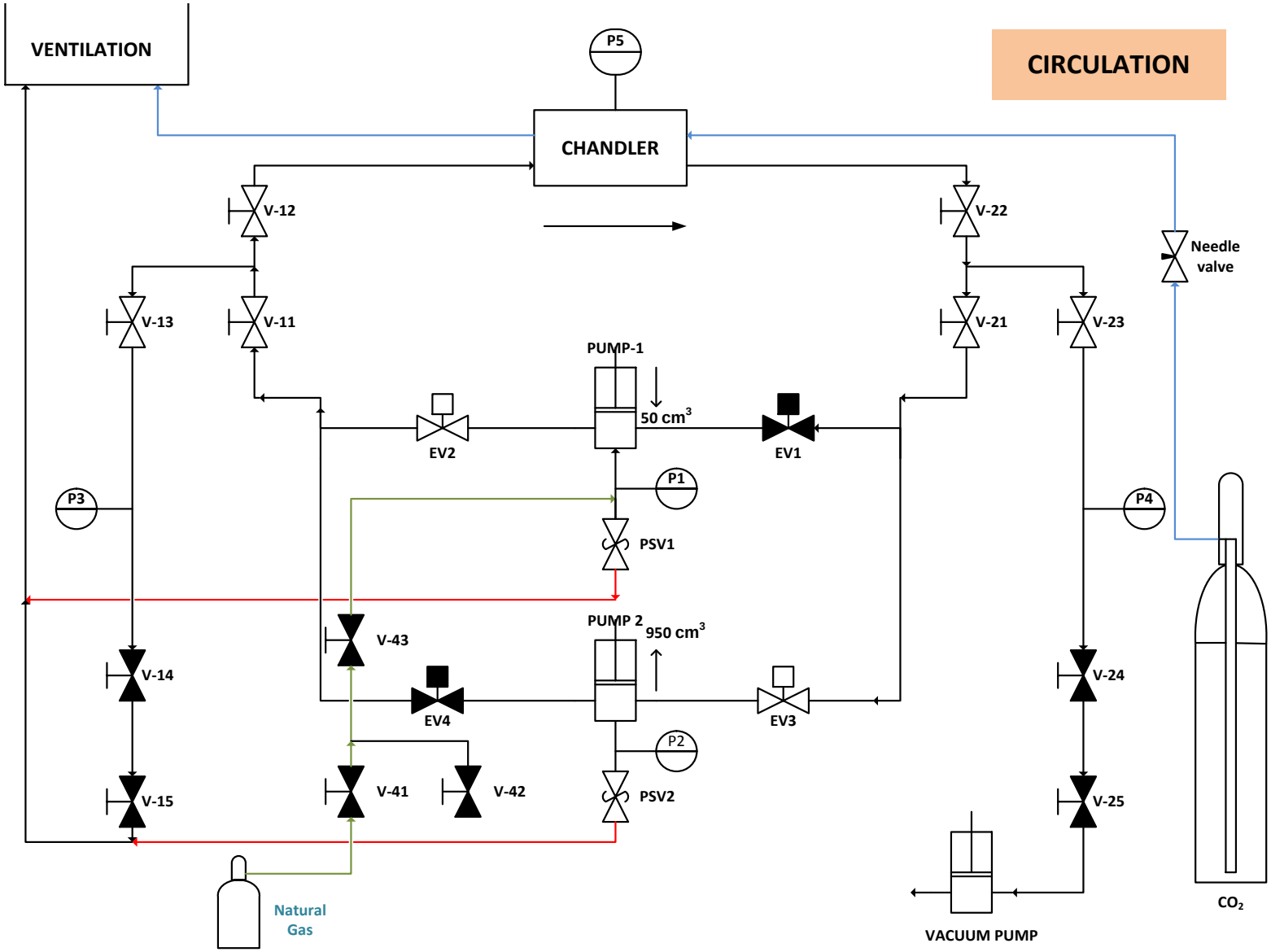

Figure 8.1: Process Flow Diagram of experimental apparatus during circulation of the gas

Proposed Procedure for GERG Dew Point Rig

Preparation day

1. Disassemble the window case. Clean the mirror and window with a dry q-tip and check the window and the O-rings for any damage. (A 2nd O-ring is placed on the back side of the mirror and should be changed annually). Replace any damaged parts and assemble back the window case. Open a new Result Sheet and store it as "TS-no". Write down on Log.
2. Make sure that the thermo element in the chandler is in contact with the back of the mirror. Put heating paste in the tip of the element.
3. Open the valve of the air system (yellow valve).
4. Set the temperature set point for the chamber, the gas line and the heating jackets of the pumps to 60°C. Make sure that the temperature stabilizes around the set points. Write down on Log.
5. Write down pressure and volume of the sample cylinder in the Result Sheet on Log.
6. Remove the level indicator from the sample cylinder.
7. Put the special fitting required in the sample side (not the one with the pressure indicator) of the sample cylinder.
8. Attach the sample cylinder to the rig with the pressure indicator (Argon side) facing down.
9. Couple the hose from the rig to the top of the sample cylinder.
10. Couple the hose from the argon bottle to the bottom of the sample cylinder. Make sure that the big valve and the small valve on the pressure regulator are closed. The pressure of the Argon bottle should always be higher than 150 bar, if not, change to a new bottle. See figure below.

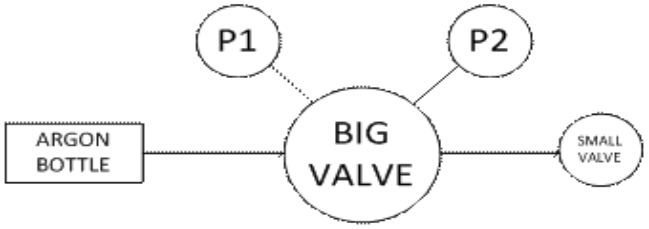

11. Turn on the pumps by pressing ON.
12. Start FALCON program and set the volume of both pumps to 950 cm^3.
13. When working with a synthetic gas, open V14 and V15, let a small amount of gas enter the rig by slowly opening the valve on the gas bottle. Repeat this 5 times (this should NOT be done when working with a sample, where the available quantity is limited)

14. Close V14 and V15.
15. Open all other valves in the rig until the sample cylinder, including EV1-EV4 via the computer program by just clicking on them.
16. Start the vacuum pump only if the rig is closed to ventilation (V14, V15 closed). Otherwise, oil from the exhaust of the vacuum pump will contaminate the rig.
17. Let the pump run over the night. Make sure that there is vacuum in the rig.

Filling-up the rig (Experimental day)

1. Note the pressure from the rig pressure sensor and the manometer on the vacuum pump. In order to have vacuum the pump should show approx. 5*10-E2 mbar.
2. Close V24 and V25 and stop the vacuum pump. Close V41 and V43 and check if the pressure in the rig is kept constant. Wait 2-3 min.
3. Set the volume of both pumps to 50 cm^3, the velocity to 2000 cm/hr and press "Start". Note down on Log.
4. Open the argon bottle.
5. Open the small valve on the argon bottle.
6. Slowly open the big valve until P2 is slightly above P3 (pressure in the sample cylinder) in order to maintain pressure inside the gas cylinder (usually 150 bar).
7. Open the lower valve (Argon side) on the sample cylinder. Check if the pressure is constant.
8. Open the upper valve (gas side) on the sample cylinder to fill the gas line from the cylinder to V1. (The moving gas hood must be above the upper valve as a precaution) (open- counter clockwise, close- clockwise)
9. Open V43 and then open very slowly V41 to fill the rig. While filling, always check that the back pressure (Argon side) of the cylinder is constant. The pressure inside the rig must be increased very slowly up to 20 bar, a little faster up to 70 bar and a little faster up to P3 (150 bar).
10. Start both pumps, set the volume to the desired value.
11. Close V41 and V43.
12. Close the valves on the top of the gas cylinder (gas side) and on the bottom of the gas cylinder (Argon side)
13. Close the Argon bottle, the big valve and the small valve of the pressure regulator (see figure 1) in this order.
14. Set the temperature set point for the chamber and the heating jackets of the pumps to 45°C. Set the set point for the gas line to ambient temperature.

15. Check if the pressure in the rig is kept pressure. Wait 5 minutes.
16. Click in the simple cycle RUN button and set the pressure to the wanted value for the first measurement.
17. Circulate the gas at a velocity of 2000 cm^3/hr for 20 minutes, to eliminate composition gradients inside the rig and evaporate gas that may have condensed during filing.

Dew Point Measurements

1. Open the CO_2 bottle (the needle valve of CO_2 must be closed).
2. Turn on the temperature device. Push AutoOFF 3 times to prevent it from turning off automatically (dAoF=deactivate Automatic off).
3. Click in the simple cycle RUN button and set the pressure to the wanted value (skip this step if it is the first measurement). Wait for the rig to stabilize at the new pressure.
4. Circulate the gas at a velocity of 2000 cm^3/hr for 10 minutes.
5. Stop the circulation by pressing Stop in the circulation menu, reduce the gas velocity to 400 cm^3/hr and press Circulate.
6. Perform the dew point measurements.
7. When the measurement is valid, write "DEW" on Comments. Three (3) valid measurements are required for each pressure.
8. Repeat all steps above to perform measurements at all required pressure levels.

Leaving the rig with pressure (pause) in order to continue the day after

1. Stop the gas circulation by pressing STOP on FOLCAN program, push the Stop Motor button and press the OFF button
2. Close the CO_2 bottle and vent the CO_2 that is remaining in the pipes.
3. Turn off the temperature device.

After the experiment is completed

1. Stop gas circulation by pressing STOP.
2. Close the valve on the CO_2 bottle and vent the CO_2 that is remaining in the pipes.
3. Turn off the temperature device.
4. Open V14, V15 and V24, V25.
5. Set the volume of both pumps at 50 cm^3.

6. When the rig is depressurized, open V41 and, then, V43. Set the volume of both pumps at 950 cm3.
7. Turn off the pumps and the computer.
8. Turn off all temperature devices.
9. Close the valve of the air system. Make sure physically that the resistance for heating the chamber is closed.
10. Close V14, V15 and V24, V25.
11. Decouple the hose from the argon bottle to the bottom of the sample cylinder carefully. Do not stand in front of it. Open the small valve slowly. Then open the big valve slowly. After the gas trapped inside is ventilated, close both valves.
12. Decouple the hose from the rig to the top of the sample cylinder. Put the cylinder to its box and take out the special fitting. Put the special stops of the valves and the level indicator back to the cylinder. Take the box to the storage area.

Appendix B: Pressure and temperature calibration

Pressure calibration

Tables B.1 to B.4 present the calibration results of manometers 1 to 4 respectively

Table B.1

P_{cal}	$P1_{read}$	ΔP*
6.54	6.61	-0.07
22.62	22.72	-0.10
52.22	52.25	-0.03
81.10	81.19	-0.09
101.69	101.76	-0.07
127.27	127.35	-0.08

Table B.2

P_{cal}	$P2_{read}$	ΔP*
6.54	6.54	0.00
22.62	22.62	0.01
52.22	52.19	0.03
81.10	81.13	-0.03
101.69	101.71	-0.02
127.27	127.30	-0.03

Table B.3

P_{cal}	$P3_{read}$	ΔP*
6.54	6.36	0.18
22.62	22.48	0.14
52.22	52.10	0.12
81.10	81.08	0.02
101.69	101.69	0.00
127.27	127.32	-0.05

Table B.4

P_{cal}	$P4_{read}$	ΔP*
6.54	6.47	0.07
22.62	22.58	0.04
52.22	52.17	0.05
81.10	81.13	-0.03
101.69	101.72	-0.03
127.27	127.34	-0.07

Temperature calibration

Table B.5: Calibration results for

T_{bath}	T_{cal}	T_{read}	Deviation
-10	-8.565	-8.375	-0.190
-5	-4.580	-4.410	-0.170
0	0.020	0.120	-0.100
5	4.930	5.050	-0.120
10	9.855	9.915	-0.060

Appendix C: Ethane data

Table C.1: Ethane data

Literature data (NIST database)		Experimental data			
		Heating (45 °C)		No heating	
P (bar)	*T (°C)*	*P (bar)*	*T (°C)*	*P (bar)*	*T (°C)*
1	-88.84	35	16.73	35	16.67
2	-74.97	35	16.75	35	16.58
3	-65.75	35	16.66	35	16.54
4	-58.63	30	9.86	30	9.48
5	-52.73	30	9.99	30	9.55
6	-47.66	30	9.82	30	9.53
7	-43.18	25	2.09	30	9.69
8	-39.14	25	1.96	25	2.27
9	-35.46	25	2.01	25	2.44
10	-32.07	20	-6.92	25	2.36
11	-28.92	20	-6.96	15	-18.31
12	-25.97	20	-6.81	15	-18.34
13	-23.19	20	-6.98	15	-18.37
14	-20.56	15	-17.57		
15	-18.07	15	-17.59		
16	-15.70	15	-17.49		
17	-13.43				
18	-11.25				
19	-9.17				
20	-7.16				
21	-5.22				
22	-3.35				
23	-1.54				
24	0.22				
25	1.92				
26	3.57				
27	5.17				
28	6.73				
29	8.25				
30	9.74				
31	11.18				
32	12.59				
33	13.97				
34	15.32				
35	16.63				
36	17.92				
37	19.18				
38	20.42				
39	21.63				
40	22.81				

Appendix D: Experimental data

Table D.1: Experimental data for SNG 2

V=600cc,T=45°C, no preheating		V=300cc,T=45°C, no preheating		V=600cc,T=35°C, no preheating		V=600cc,T=45°C, preheating	
P (bar)	*T (°C)*	*P (bar)*	*T (°C)*	*P (bar)*	*T (°C)*	*P (bar)*	*T (°C)*
80	-17.1	88	-37.5	85	-33.6	80	-25.0
80	-17.1	88	-37.6	85	-33.5	80	-25.2
80	-17.2	88	-37.4	85	-33.6	80	-25.2
70	-8.6	85	-31.6	87	-37.6	70	-17.8
70	-8.7	85	-31.6	87	-37.4	70	-17.9
70	-8.7	85	-31.5	87	-38.0	70	-17.8
60	-8.6	80	-25.3	87	-37.9	60	-12.5
60	-8.5	80	-25.3	80	-25.5	60	-12.5
60	-8.6	80	-25.4	80	-25.6	60	-12.3
50	-6.4	75	-21.7	80	-25.7	50	-8.5
50	-6.4	75	-21.6	80	-25.8	50	-8.8
50	-6.4	75	-21.5	75	-22.3	50	-8.6
50	-5.6	70	-17.3	75	-22.3	40	-6.5
50	-5.7	70	-17.4	75	-22.4	40	-6.5
50	-5.6	70	-17.2	70	-18.8	40	-6.4
40	-12.4	60	-13.2	70	-18.7	30	-5.8
40	-12.5	60	-13.2	70	-18.8	30	-5.8
40	-12.5	60	-13.1	60	-13.3	30	-5.9
30	-25.4	50	-9.4	60	-13.3		
30	-25.5	50	-9.3	60	-13.3		
30	-25.5	50	-9.4	50	-9.6		
		40	-7.1	50	-9.4		
		40	-7.1	50	-9.5		
		40	-7.2	40	-7.1		
		30	-6.3	40	-7.1		
		30	-6.4	40	-7.1		
		30	-6.3	30	-6.2		
		20	-7.7	30	-6.3		
		20	-7.6	30	-6.2		
		20	-7.7				
		15	-9.7				
		15	-9.8				
		15	-9.5				
		10	-13.4				
		10	-13.3				
		10	-13.4				

Table D.2: Experimental data for SNG 3

1st measurement		*2nd measurement*							
V=600cc,T=45°C, no preheating		V=600cc,T=45°C, no preheating		V=300cc, T=45°C, no preheating		V=600cc, T=35°C, no preheating		V=300cc, T=45°C, preheating	
P (bar)	*T (°C)*	*P (bar)*	*T (°C)*	*P (bar)*	*T (°C)*	*P (bar)*	*T (°C)*	*P (bar)*	*T (°C)*
92	-21.9	94	-25.2	93	-24.1	93	-25.1	95	-27.7
92	-22.0	94	-25.4	93	-24.0	93	-25.3	95	-28.0
92	-21.9	94	-25.5	93	-23.8	93	-25.4	95	-28.0
80	-11.8	94	-25.6	93	-24.0	90	-20.2	90	-20.1
80	-11.8	90	-19.7	90	-18.5	90	-20.3	90	-20.1
80	-11.5	90	-19.6	90	-18.4	90	-20.4	90	-20.2
70	-7.0	90	-19.9	90	-18.7	90	-20.4	80	-12.6
70	-7.0	80	-11.8	80	-11.6	80	-12.7	80	-12.6
70	-7.1	80	-11.7	80	-11.4	80	-12.7	80	-12.7
60	-3.9	80	-12.0	80	-11.5	80	-12.4	80	-12.7
60	-4.2	80	-12.0	70	-7.9	70	-8.0	70	-7.7
60	-4.1	70	-7.2	70	-7.5	70	-7.9	70	-7.7
60	-4.1	70	-7.2	70	-7.6	70	-8.0	70	-7.7
50	-2.1	70	-7.4	60	-4.6	60	-4.4	60	-4.3
50	-2.2	60	-4.1	60	-4.5	60	-4.5	60	-4.3
50	-2.1	60	-4.1	60	-4.5	60	-4.6	60	-4.4
40	-1.2	60	-4.0	50	-2.6	50	-2.5	50	-2.6
40	-1.3	60	-4.0	50	-2.6	50	-2.5	50	-2.6
40	-1.3	50	-2.3	50	-2.6	50	-2.6	50	-2.4
		50	-2.3	40	-1.8	40	-1.8	40	-1.9
		50	-2.3	40	-1.7	40	-1.7	40	-1.8
		40	-1.5	40	-1.8	40	-1.7	40	-1.7
		40	-1.6	30	-2.5	30	-2.5		
		40	-1.5	30	-2.6	30	-2.4		
		30	-2.2	30	-2.6				
		30	-2.1						
		30	-2.1						

Table D.1: Experimental data for RG 1

1st measurement		*2nd measurement*					
V=600cc,T=45°C, no preheating		V=600cc,T=45°C, no reheating		V=300cc,T=45°C, no preheating		V=600cc,T=35°C, no preheating	
P (bar)	*T (°C)*	*P (bar)*	*T (°C)*	*P (bar)*	*T (°C)*	*P (bar)*	*T (°C)*
105	0.6	105	1.2	105	1.2	105	-1.4
105	0.7	105	1.0	105	1.3	105	-1.7
105	0.4	105	1.0	105	1.3	105	-1.9
105	0.5	100	8.7	100	8.3	105	-0.9
100	8.2	100	8.6	100	8.2	105	-1.1
100	8.2	100	8.4	100	8.2	105	-1.2
100	8.1	90	15.8	80	20.1	100	6.5
90	15.6	90	15.7	80	20.1	100	6.4
90	15.6	90	15.5	80	20.2	100	6.3
90	15.7	90	15.5	60	24.5	90	14.4
80	19.7	80	19.9	60	24.5	90	14.4
80	19.7	80	19.8	60	24.4	90	14.4
80	19.7	80	19.9	40	23.6	80	18.6
70	22.1	70	22.5	40	23.6	80	18.5
70	22.1	70	22.6	40	23.7	80	18.4
70	22.1	70	22.5	40	23.7	70	21.2
60	23.8	60	23.9			70	21.1
60	23.8	60	23.9			70	21.1
60	23.9	60	23.9			60	22.9
50	24.6	50	24.5			60	22.8
50	24.5	50	24.5			60	22.8
50	24.5	50	24.5			50	23.3
						50	23.3
						50	23.4

Appendix E: Predicted dew points from modelling

Table E.1: Predicted dew points from modelling for SNG 2

SRK		PC-SAFT		UMR-PRU	
P (bar)	*T (°C)*	*P (bar)*	*T (°C)*	*P (bar)*	*T (°C)*
1.00	-38.60	2.03	-30.57	5.00	-21.76
1.64	-33.15	4.29	-21.95	6.49	-18.72
1.65	-33.11	9.08	-13.66	7.97	-16.37
2.72	-27.45	19.23	-7.17	9.46	-14.48
5.75	-18.94	30.01	-5.56	10.94	-12.91
9.89	-13.15	40.70	-6.68	12.43	-11.60
12.18	-11.14	59.22	-13.00	13.91	-10.50
20.27	-7.24	79.13	-30.35	15.40	-9.55
25.79	-6.25	82.25	-41.71	16.89	-8.74
31.04	-5.97	80.75	-49.87	18.37	-8.05
40.53	-6.99	66.79	-68.30	19.86	-7.45
54.60	-11.77	63.70	-70.86	21.34	-6.94
57.49	-13.15	60.74	-73.11	22.83	-6.51
60.80	-14.96	56.57	-76.04	24.31	-6.15
65.86	-18.31	52.68	-78.55	25.80	-5.85
76.38	-29.47	49.06	-80.74	27.29	-5.60
78.26	-33.15	45.69	-82.68	28.77	-5.41
80.17	-42.41	45.29	-82.90	30.26	-5.27
79.56	-47.79	45.14	-82.99	31.74	-5.17
77.73	-53.15	45.06	-83.03	33.23	-5.11
69.33	-65.02	45.04	-83.04	34.71	-5.09
60.80	-72.57			49.54	-6.74
60.02	-73.15			55.97	-8.38
52.57	-78.10			60.88	-10.03
49.06	-80.21			64.94	-11.67
45.78	-82.06			68.41	-13.31
45.68	-82.11			71.44	-14.96
45.63	-82.14			74.10	-16.60
45.60	-82.15			76.44	-18.25
				78.51	-19.89
				80.33	-21.54
				81.93	-23.18
				83.32	-24.83
				84.51	-26.47
				85.52	-28.12
				86.36	-29.76
				87.03	-31.41
				87.54	-33.05
				87.90	-34.70
				88.11	-36.34
				88.18	-37.99

Table E.2: Predicted dew points from modelling for SNG 3

SRK		PC-SAFT		UMR-PRU	
P (bar)	*T (°C)*	*P (bar)*	*T (°C)*	*P (bar)*	*T (°C)*
2.03	-31.51	1.00	-39.55	5.00	-22.70
3.34	-25.73	1.65	-34.16	6.70	-19.16
5.51	-19.81	1.81	-33.15	8.41	-16.45
9.08	-13.93	2.72	-28.52	10.11	-14.29
14.82	-8.56	5.75	-19.72	11.82	-12.51
23.79	-4.34	10.09	-13.15	13.52	-11.03
37.17	-2.39	12.18	-11.04	15.23	-9.77
38.42	-2.38	20.27	-5.97	16.93	-8.70
55.30	-4.39	25.23	-4.30	18.64	-7.78
69.90	-9.44	37.81	-2.78	20.34	-6.99
80.04	-15.80	40.53	-2.85	22.05	-6.32
85.95	-22.43	49.16	-3.82	23.75	-5.74
88.52	-28.71	59.60	-6.51	25.46	-5.25
88.89	-32.30	60.80	-6.93	27.16	-4.83
88.77	-34.31	68.24	-10.24	28.87	-4.49
87.66	-39.10	73.03	-13.15	30.57	-4.21
85.88	-43.11	74.93	-14.55	32.27	-3.99
83.87	-46.42	79.76	-19.09	33.98	-3.82
81.87	-49.16	81.06	-20.71	35.68	-3.70
79.97	-51.48	82.94	-23.61	37.39	-3.64
78.19	-53.47	84.77	-27.93	39.09	-3.62
76.53	-55.25	85.64	-33.15	53.75	-5.09
74.94	-56.86	85.66	-33.83	59.99	-6.57
73.40	-58.38	85.66	-33.89	64.72	-8.05
72.97	-58.80	85.08	-38.92	68.61	-9.52
		83.68	-43.21	71.93	-11.00
		81.89	-46.82	74.81	-12.48
		81.06	-48.19	77.33	-13.95
		79.95	-49.85	79.55	-15.43
		78.01	-52.43	81.50	-16.91
		77.42	-53.15	83.22	-18.39
		76.13	-54.64	84.73	-19.86
		74.36	-56.56	86.04	-21.34
		72.69	-58.25	87.16	-22.82
		71.14	-59.75	88.11	-24.29
		69.93	-60.89	88.90	-25.77
		69.35	-61.43	89.53	-27.25
		68.79	-61.94	90.01	-28.72
		67.70	-62.93	90.34	-30.20
		66.14	-64.31	90.54	-31.68
		64.65	-65.63	90.61	-33.16
		63.17	-66.92		
		60.92	-68.90		
		60.80	-69.00		

SRK		PC-SAFT		UMR-PRU	
P (bar)	*T (°C)*	*P (bar)*	*T (°C)*	*P (bar)*	*T (°C)*
		57.30	-72.05		
		56.05	-73.15		
		53.36	-75.51		
		49.14	-79.26		
		44.74	-83.27		
		40.53	-87.25		
		40.27	-87.50		
		34.68	-93.15		
		33.70	-94.19		
		24.77	-104.62		
		20.27	-110.83		
		18.73	-113.15		
		17.48	-115.13		
		11.97	-125.30		
		8.65	-133.15		
		8.02	-134.87		
		5.31	-143.69		
		3.49	-151.71		
		3.22	-153.15		
		2.29	-158.96		
		1.50	-165.49		

Table E.2: Predicted dew points from modelling for RG 1

SRK		PC-SAFT		UMR-PRU	
P (bar)	*T (°C)*	*P (bar)*	*T (°C)*	*P (bar)*	*T (°C)*
2.03	-12.68	1.00	-21.20	5.00	-2.60
3.34	-5.97	1.65	-15.08	7.18	2.79
5.51	1.07	1.92	-13.15	9.37	6.77
8.99	8.19	2.72	-8.55	11.55	9.89
14.48	15.03	5.75	1.96	13.73	12.42
22.89	21.06	8.04	6.85	15.92	14.52
35.25	25.40	12.02	12.74	18.10	16.30
48.59	26.78	20.27	20.03	20.28	17.80
49.24	26.79	24.48	22.37	22.47	19.09
61.68	25.83	40.32	26.85	24.65	20.20
73.54	23.13	40.53	26.88	26.83	21.15
83.55	19.22	47.21	27.33	29.02	21.96
91.42	14.55	48.44	27.34	31.20	22.65
97.14	9.49	56.84	26.85	33.38	23.24
100.88	4.29	60.80	26.28	35.57	23.72
102.92	-0.84	69.39	24.27	37.75	24.12
103.59	-5.76	81.06	19.50	39.93	24.43
103.59	-6.15	86.27	16.31	42.12	24.67
103.20	-10.40	95.96	6.85	44.30	24.83
102.03	-14.72	96.42	6.18	46.48	24.93

99.35	-20.56	100.75	-4.08	48.67	24.96
96.06	-25.68	101.29	-9.41	65.27	23.26
92.54	-30.17	101.03	-13.15	72.21	21.56
89.73	-33.34	101.00	-13.34	77.42	19.85
2.03	-12.68	98.74	-21.23	81.68	18.15
3.34	-5.97	95.10	-27.83	85.30	16.45
5.51	1.07	91.00	-33.15	88.42	14.74
8.99	8.19	90.85	-33.33	91.14	13.04
14.48	15.03	86.74	-37.70	93.52	11.34
22.89	21.06	84.72	-39.64	95.62	9.63
35.25	25.40	81.06	-42.93	97.46	7.93
48.59	26.78	79.09	-44.61	99.06	6.23
49.24	26.79	74.16	-48.67	100.45	4.52
61.68	25.83	69.76	-52.19	101.64	2.82
73.54	23.13	68.56	-53.15	102.64	1.12
83.55	19.22	65.65	-55.47	103.47	-0.59
91.42	14.55	61.59	-58.75	104.13	-2.29
97.14	9.49	60.80	-59.40	104.63	-3.99
100.88	4.29	57.50	-62.12	104.98	-5.70
102.92	-0.84	53.36	-65.63	105.19	-7.40
103.59	-5.76	49.20	-69.26	105.25	-9.10
103.59	-6.15	44.92	-73.15		
103.20	-10.40	43.04	-74.91		
102.03	-14.72	40.53	-77.33		
99.35	-20.56	34.32	-83.69		
96.06	-25.68	26.60	-92.63		
92.54	-30.17	26.19	-93.15		
89.73	-33.34	20.27	-101.26		
		19.52	-102.38		
		13.96	-111.84		
		13.29	-113.15		
		9.77	-120.85		
		6.72	-129.30		
		5.58	-133.15		
		4.55	-137.14		
		3.05	-144.38		
		2.03	-151.02		
		1.76	-153.15		
		1.34	-157.10		

Appendix F: Certified uncertainties of GC analysis

Table F.1: Certified Uncertainty of GC analysis for SNG 2

Component	Uncertainty relative %
n-heptane	3
methane	1

Table F.2: Certified Uncertainty of GC analysis for SNG 3

Component	Uncertainty relative %
n-octane	2
n-heptane	2
n-hexane	1
n-pentane	1
isopentane	1
n-butane	1
carbon dioxide	1
propane	1
nitrogen	1
ethane	1
methane	0.5